Fault and natural fracture control on upward fluid migration: insights from a shale gas play in the St. Lawrence Platform, Canada

Ladevèze, P. [1,a,b], *Rivard, C.* [b], *Lavoie, D.*[b], *Séjourné, S.*[c], *Lefebvre, R.*[a], *Bordeleau G.*[b]

[a] *INRS, Centre Eau Terre Environnement, 490 rue de la Couronne, Quebec City, QC G1K 9A9, Canada*

[b] *Geological Survey of Canada – Quebec, 490 rue de la Couronne, Quebec City, QC G1K 9A9, Canada*

[c] *Enki GéoSolutions, Montréal, Canada*

[1] *Corresponding author: pierrelad@gmail.com*

Abstract

Environmental concerns have been raised with respect to shale gas exploration and production, especially in eastern Canada and northeastern United States. One of the major public concerns has been the contamination of fresh water resources. This paper focuses on the investigation of possible fluid upward migration through structural features in the intermediate zone (IZ), located between a deep shale gas reservoir and shallow aquifers. The approach provides insights into how such an investigation can be done when few data are available at depth. The study area is located in the shale dominated succession of the St. Lawrence Platform (eastern Canada), where the Utica Shale was explored for natural gas between 2006 and 2010. Detailed analyses were carried out on both shallow and deep geophysical log datasets providing the structural attributes and preliminary estimates of the hydraulic properties of faults and fractures. Results show that the active groundwater flow zone is located within the upper 60 m of bedrock, where fractures are well interconnected. Fractures from one set were found to be frequently open in the IZ and reservoir, providing a poorly connected network. The fault zones are here described as combined conduit-barrier systems with sealed cores and some open fractures in the damage zones. Although no direct hydraulic data were available at depth, the possibility that the fracture network or fault zones act as large-scale flow pathways seems very unlikely. A conceptual model of the fluid flow patterns summarizing the current understanding of the system hydrodynamics is also presented.

255 words

Keywords: natural fractures; faults; upward fluid migration; shale gas; St. Lawrence Platform

1 Introduction

Shale gas development in North America has raised strong local environmental concerns, largely in relation to potential contamination of fresh water resources during hydraulic fracturation operations (BAPE 2014; CCA 2014; EPA 2016). One of these concerns is associated with potential upward fluid migration from deep geological reservoirs to shallow aquifers through preferential pathways such as natural fractures and faults (Lefebvre 2016). Fluids of concerns include hydraulic fracturing fluids, gases (mostly methane) and formation brines (Birdsell *et al.* 2015). Although the presence of natural preferential pathways that could affect fresh water quality is of particular anxiety to the population, it is now recognized among the experts that the well casing integrity is the major concern with respect to potential upward fluid migration (Dusseault and Jackson 2014; Lefebvre 2016). Nonetheless, the need for a better description and representation of the potential preferential flow pathways in hydrogeological models to assess the risk of upward fluid migration has been stressed by many researchers (Gassiat *et al.* 2013; Kissinger *et al.* 2013; Birdsell *et al.* 2015; Reagan *et al.* 2015; Grasby *et al.* 2016). So far, most authors have used mean values to obtain representations of different hydrogeological systems for their simulations. While these provide interesting insights into mechanisms and conditions that could lead to aquifer contamination, there is a critical need for field-based research studies in developing a methodology aimed at identifying natural preferential migration pathways using multiple data sets (Jackson *et al.* 2013). In particular, very little work has focused on the characterization of fracture networks in the intermediate zone (IZ), which is located between shallow aquifers (usually in the upper 200 m) used for water supply and deep hydrocarbon reservoirs (usually deeper than 1000 m). However, this geological interval controls the shallow aquifer vulnerability to activities carried out at depth.

In the St. Lawrence Platform (Quebec, Canada), shale gas exploration targeting the Utica Shale was conducted between 2006 and 2010 until a *de facto* moratorium on hydraulic fracturing came into force, in response to strong environmental concerns (BAPE 2014). In this context, the objective of this study was to identify the potential for fluid upward migration through natural fractures and faults in the Saint-Édouard area, 65 km south-west of Quebec City (Fig. 1), a region where a promising shale gas well had been drilled.

Multisource data including shallow and deep log datasets, core data and seismic data were examined to assess the geometry and potential hydraulic properties of the structural features that affect the sedimentary succession, including the IZ. A special focus was placed on the presence and properties of open fractures and permeable faults. Because hydraulic data are currently not available in the study area for depths below surficial aquifers, as is the case in most shale gas plays, this paper discusses how existing common field datasets can help to understand the hydraulic behavior of the fractures and faults that cut through a sedimentary succession. A precise quantitative assessment of the hydraulic properties of these structural discontinuities is beyond the scope of the paper. Our approach rather provides semi-quantitative insights into the possibility of upward migration through fractures and faults, based on available field observations and knowledge acquired from the geological context.

2 The St. Lawrence Platform and St-Édouard study area

2.1 Regional geological setting

The St. Lawrence sedimentary Platform is divided into two tectonostratigraphic domains (St-Julien and Hubert 1975): the autochthonous and the parautochthonous domains (Fig. 1). In this paper, the term St. Lawrence Platform (SLP) refers to the area roughly located between Montreal and Quebec City (Province of Quebec, Canada).

In the autochthonous domain, Cambrian-Lower Ordovician clastic and carbonate units of the Potsdam and Beekmantown groups unconformably overly the Grenvillian crystalline rocks (Lavoie *et al.* 2012). During the Middle to Late Ordovician, these units were overlain by the carbonate units of the Chazy, Black River and Trenton groups and by the calcareous shale of the Utica Shale (Lavoie 2008). The uppermost preserved units of the SLP consist of the Upper Ordovician turbidite deposits of the Lorraine Group and the molasse units of the Queenston Group. The Sainte-Rosalie, Lorraine and Queenston groups were slightly deformed in the regional-scale Chambly-Fortierville syncline. A normal fault system also intersects the units throughout the autochthonous domain (Rivière Jacques-Cartier fault) (Fig. 1).

The parautochthonous domain corresponds to rocks that were displaced in a southeast-dipping system of thrust faults that display imbricated thrust fan geometries (St-Julien *et al.* 1983; Séjourné *et al.* 2003; Castonguay *et al.* 2006). The parautochthonous units were also deformed by some northeast-striking folds. The Aston fault and the Logan’s Line regional thrust-faults delimit the parautochthonous domain to the NE and SW, respectively (St-Julien and Hubert 1975; Globensky 1987). The Logan’s Line represents the structural limit between the SLP (or parautochthonous domain) and the Appalachians (or the allochthonous domain) where rocks were displaced northwestwardly along the Appalachian’s thrust planes (Tremblay and Pinet 2016). In the Saint-Édouard area, recent seismic reinterpretation of vintage industry data (Konstantinovskaya *et al.* 2009; Lavoie *et al.* 2016) showed that the parautochthonous domain forms a triangular zone delimited by a NW-dipping backthrust to the northwest and by a SE-dipping thrust fault to the southeast (Logan’s Line) (Fig. 1).

The Utica Shale is considered an excellent conventional hydrocarbon source rock and an unconventional gas reservoir (Lavoie *et al.* 2008; Lavoie *et al.* 2014). It is mostly overlain by the fine-grained units of the Lorraine Group and it is laterally equivalent to the Lotbinière Formation in the northern part of the autochthonous domain, while it is structurally overlain by the Les Fonds Formation in the parautochthonous domain (Fig. 1). The Lotbinière and Les Fonds formations (Fig. 2) display a dominant lithofacies similar to, and are also time-correlative with, the Utica Shale (Lavoie *et al.* 2016). However, Lorraine Group units are made of gray to dark-grey shales with metre- to centimetre-thick siltstone interbeds (Clark and Globensky 1973; Globensky 1987). Shales from the Lorraine Group are more clayey than those of the Utica Shale (Lavoie *et al.* 2008). The siltstone interbeds are mostly concentrated in the upper part of the Nicolet Formation (Lorraine Group) (Clark 1964; Clark and Globensky 1973; Séjourné *et al.* 2013). The maximum thickness of these siltstone-rich successions is unknown. Field observations showed that the siltstone-rich zones are locally concentrated in recurring multiple intervals that display thicknesses of up to 15-20 m in the upper part of the formation (Fig. 2). The siltstone proportion decreases with depth, from up to 80% of siltstones in the upper part of the unit, to 30-40% in the middle part, to almost no siltstone interbeds at the base of that formation (Séjourné *et al.* 2013). Given the limited outcrop availability and the lack of clear marker beds, the lateral extension of these interbeds in the shale-dominated succession is largely unknown.

The stratigraphic (sensu stricto) intermediate zone is provided by the fine-grained clastics of the Lorraine Group and also by the Utica Shale time- and facies correlative Lotbinière and Les Fonds formations to the north and south, respectively.

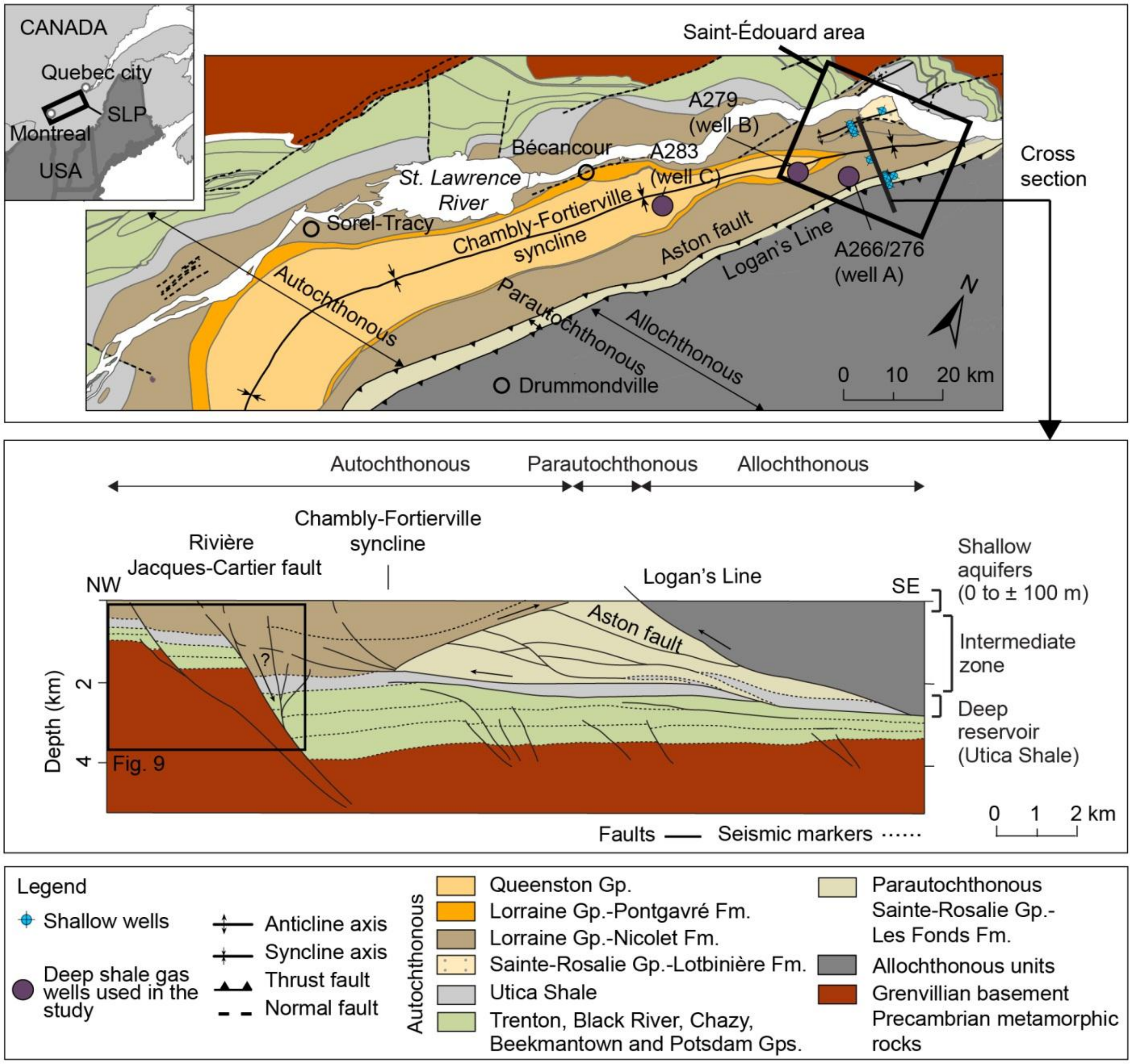

Fig. 1 Location of the study area and its geological context (geological maps adapted from Clark and Globensky (1973); Globensky (1987); Slivitzky and St-Julien (1987); Thériault and Beauséjour (2012); Konstantinovskaya *et al.* (2014a). Gp.: Group; Fm.: Formation; SLP: St. Lawrence Platform. The structural cross-section is from Lavoie *et al.* (2016) that is based on vintage industry data.

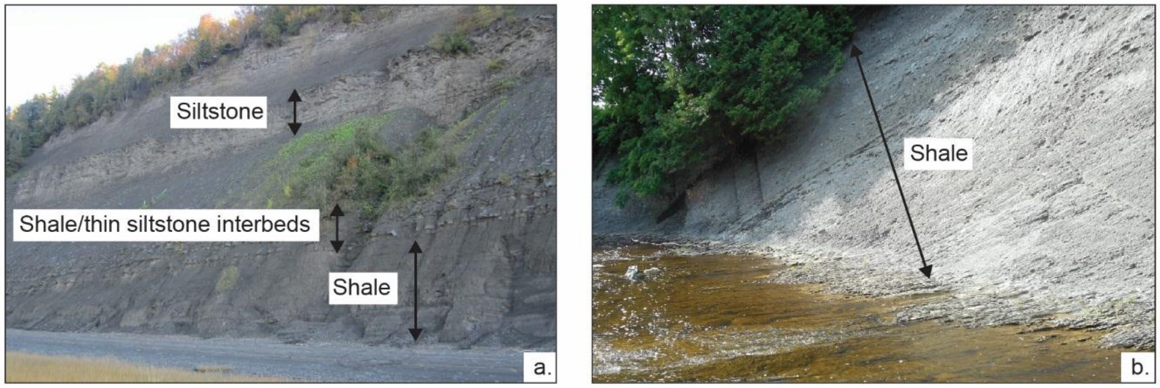

Fig. 2 Examples of outcropping IZ units of the Saint-Édouard area: **a**. Lorraine Group (Nicolet Formation): grey-black shales with thick siltstone interbeds and **b**. Les Fonds Formation: black shales.

2.2 Conceptual models of the natural fracture network

Conceptual models of the fracture network that affects the geological units of the Saint-Édouard area were proposed in Ladevèze *et al.* (2018) (Fig. 3). These models are based on observations made in 15 outcrops of various orientations, as well as in 11 shallow observation wells and 3 deep shale gas wells. Three sets of high-angle fractures were identified: F1, F2 and F3, their numbering is based on their relative timing (F1 is the oldest). Bedding parallel fractures were also observed in the shallow interval. The F1 and F2 fractures strike respectively NE and NW, are perpendicular to each other and orthogonally crosscut the bedding planes. They can be found everywhere throughout the shallow and deep intervals. The third fracture set (F3) strikes WNW and is sub-vertical (dip>80°), irrespective of the bedding plane attitudes. F3 fractures are more sparsely distributed and were mostly observed in the Utica Shale. Higher fracture densities were found in the deep reservoir compared to the lower portion of the IZ where some log data are available from shale gas wells (Fig. 3a and b). Based on the similarities of the fracture sets and knowledge of the geologic history of the region, it was concluded that shallow and deep fracture datasets could be used as analogs for the intermediate zone for which very little data are available.

In siltstone units, fractures are stratabound, contrary to those in shale units. Fracture densities are also higher in siltstone units (compared to shale units) and in the calcareous Utica Shale (compared to the more clayey Lorraine Group units). This can be related to their relative difference in brittleness (Séjourné 2017; Ladevèze *et al.* 2018).

To summarize and integrate all the information and knowledge acquired on the fracture network, representative elementary volumes (REV) were proposed for the different geological intervals (Fig. 3a and b) and for the shale and siltstone units (Fig. 3c and d). The sizes of the REVs were defined based on fracture length and spacing in the shale and siltstone units (Lorraine Group) of the area as originally proposed in Oda (1985, 1988) and Odling *et al.* (1999). It must be kept in mind that these REVs are theoretical volumes that are considered representative of a given unit based on available fracture data.

There is a lack of field evidence for the vertical extent of structural discontinuities due to the limited size of the outcrops and to the fact that borehole data do not provide any direct observation of fracture lengths (Ladevèze *et al.* 2018). Due to these limitations, and the near absence of data for the intermediate zone, the vertical extension of natural fractures, which represents a critical parameter to assess aquifer vulnerability, still remains elusive (Ladevèze *et al.* 2018).

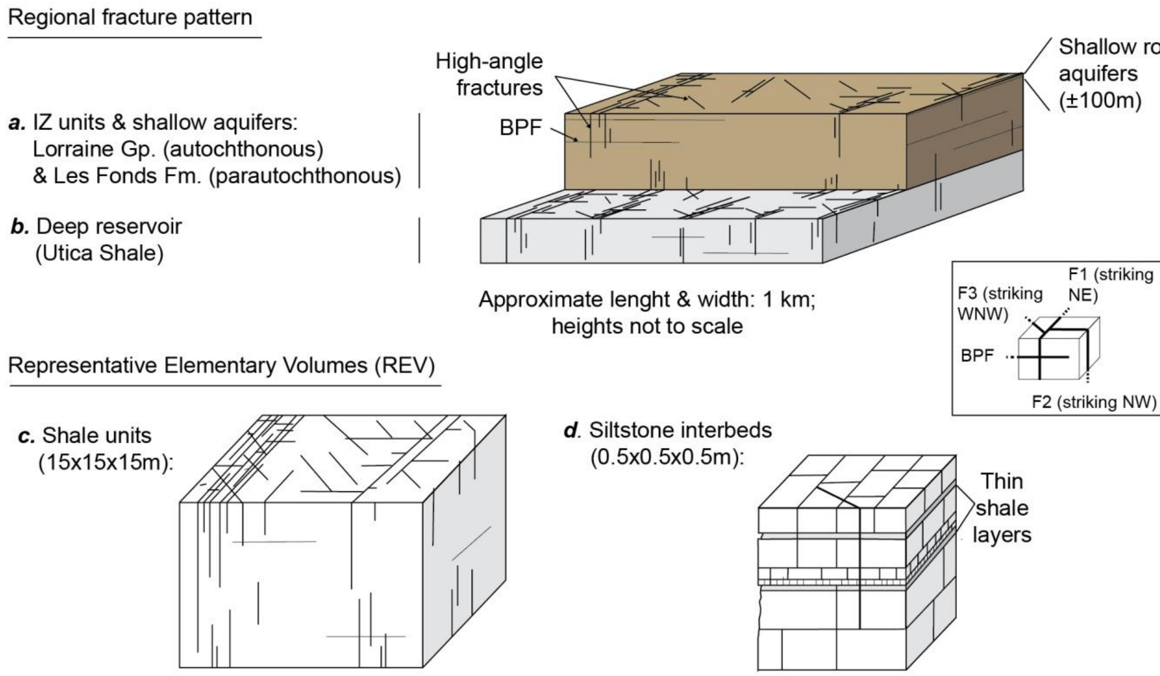

Fig. 3 Conceptual models of the fracture network in the Saint-Édouard area. The regional fracture pattern is represented in **a**. for the shallow aquifers and intermediate zone (IZ) units; in **b.** for the deep reservoir. The fracture pattern is also represented using REVs at a much more local scale for: **c**. shale units and **d**. siltstone interbeds. BPF: Bedding-parallel fractures; F1, F2 and F3: high-angle fracture sets; the numeration is based on the relative timing of the fracture sets formation. Figure modified from Ladevèze *et al.* (2018).

2.3 Key elements for the hydrogeological context

In the Saint-Édouard area, bedrock hydraulic conductivities (*K*) vary between 10^{-5} and 10^{-9} m/s according to pneumatic slug tests carried out on 11 shallow wells (open to bedrock) (Ladevèze *et al.* 2016). Higher *K* values were obtained in wells located in the autochthonous domain, with a marked correlation associated with the presence of siltstone interbeds. Wells in the parautochthonous domain displayed lower *K* values, as they only intersected shale units that are highly folded and faulted.

The occurrence of brines migrating into the shallow aquifer was documented in the vicinity of the Rivière Jacques-Cartier normal fault (Fig. 1) (Bordeleau *et al.* 2018a; Bordeleau *et al.* 2018b). The authors indicated that the presence of this brine in a few shallow (50 m) wells does not necessarily point to the existence of a large-scale upward migration pathway from the gas reservoir. This brine contribution would rather result from regional groundwater flow originating in the Appalachian uplands and circulating at a maximum depth of a few hundred meters. Hence, groundwater would flow, at least to some extent, into formations containing old saline water, then discharge in the vicinity of the Rivière Jacques-Cartier fault system (Bordeleau *et al.* 2018b). The concentrations of thermogenic methane measured in wells close to this normal fault were not higher than those in wells located elsewhere in the region and its isotopic composition was different than that of the Utica Shale (Bordeleau *et al*. 2018b). The thermogenic gas occurrences in the shallow aquifer of the Saint-Édouard area are interpreted to be sourced from the shallow shale units themselves (thermogenic gas being trapped in pores) (Lavoie *et al.* 2016; Bordeleau *et al.* 2018b).

3 Methodology

A three-step methodology was employed in this study. First, the presence and potential properties of open natural fractures within the intermediate zone was assessed to the best of our knowledge given the available data, to evaluate their impact on groundwater flow dynamics. Second, the architecture and properties of the regional fault zones were examined to infer their hydraulic properties, in order to assess their hydraulic behavior (for instance, whether they are permeable or not). Finally, the acquired information was gathered to assess, semi-quantitatively, the potential for upward fluid migration from the shale gas reservoir to the shallow aquifer based on available field data.

The general term “fracture” encompasses a large number of structures (Peacock *et al.* 2016). Here, the term “fractures” refers to meter scale planar discontinuities within the rock mass without visible displacement. To the contrary, the term “faults” here refers to discontinuities that show a displacement. In the SLP, faults were defined both at a local (meter) and a regional (kilometer) scale.

3.1 Data collection

In this study, the focus was placed on structural features that could act as preferential upward fluid flow pathways. In this perspective, fracture and fault physical properties (aperture, cementation), cross-cutting relationships and extent/distribution were carefully examined using all available data. For the Saint-Édouard area, the datasets comprised data from field observations and measurements, core samples, digital logs (shallow and deep wells) and seismic profiles.

A total of 15 shallow (from 15 to 145 m within the shallow fractured rock aquifer) observation wells were drilled into the Lorraine and Sainte-Rosalie groups (Ladevèze *et al.* 2016), of which 11 were logged using acoustic and optical televiewer tools (Crow and Ladevèze 2015). Core samples were also collected in seven of these boreholes. To complete the dataset at greater depth in the sedimentary succession, Formation Micro Imager (FMI) logs acquired in three deep shale gas wells: well A (A266/A276 - Leclercville n°1), B (A279 - Fortierville n°1) and C (A283 - Ste-Gertrude n°1) (see Fig. 1 for their location). The FMI logs were recorded in both the vertical and horizontal portions of the three studied shale gas wells. The logged intervals (true vertical depth) range from 1470 to 2010 m for well A, 560 to 2430 m for well B and 590 to 2010 m for well C. These intervals include the Utica Shale and variable portions of the overlying Lorraine Group. In the horizontal portion of these wells ("horizontal legs"), the logged intervals span across 1000, 970 and 920 m in the Utica Shale, respectively. These horizontal portions, also in true vertical depths, were drilled approximatively between 1900-1950, 2150-2250 and 1800-1850 m below the ground surface for wells A, B and C respectively. These FMI logs were provided by industry.

3.2 Characterization of open fractures

3.2.1 General approach

The Lorraine Group and the Utica Shale have low matrix porosity (geometric mean total porosity ~2.9%; BAPE 2010; Nowamooz *et al.* 2013; Séjourné *et al.* 2013; Séjourné 2015) and permeability (geometric mean permeability: 10^{-20} m^2, i.e., 10^{-5} mD or milliDarcy; BAPE 2010 and Séjourné *et al.* 2013). As the matrix of these shales is very tight (Haeri-Ardakani *et al.* 2015; Lavoie *et al.* 2016; Chen *et al.* 2017), it appears that significant fluid flow circulation could only occur through open fractures. The presence of open fractures in the rock mass was thus investigated using the conceptual models of the fracture network developed in Ladevèze *et al.* (2018) (Fig. 3) with the aim of identifying potential flow pathways.

The main characteristics of the natural fractures within the study area that could impact fluid migration are summarized in Table 1. These characteristics should be taken into consideration in assessment studies investigating potential upward migration.

Table 1 Summary of natural fracture network characteristics in the intermediate zone (IZ) that may either enhance or limit upward fluid migration

Natural fracture characteristics that were examined	Enhance fluid migration	Limit fluid migration
Open fractures	Confirmed presence, especially open frac-	Open fractures are parallel to one another:

		tures in multiple sets	limited interconnection
Open fractures attributes	Fracture sets versus contemporary *in situ* SH_{max} (maximum horizontal stress) orientations	Fracture planes are parallel to SH_{max}	Fracture planes are orthogonal to SH_{max}
	Distribution of open fractures in the sedimentary succession	High density of open fractures	Sparsely distributed open fractures
	Fracture aperture in the deep intervals (reservoir and IZ)	Large apertures	Small apertures
Open fractures and hydraulic properties of the rock mass	Fracture porosity in a context of low matrix porosity rock	High fracture porosity	Low fracture porosity
	Fracture permeability (k)	High fracture *k*	Low fracture *k*

3.2.2 Open fracture attributes

Open fractures were identified in shallow observation wells and in both vertical and horizontal sections of the deep shale gas wells. Fracture observations are, however, affected by an important sampling bias related to their orientation versus that of the borehole (sub-vertical fractures are under-sampled by vertical wells). Another important bias is that fracture aperture may be enhanced and closed natural fracture planes artificially opened during drilling operations (due to the rotation of the drill bit, to the injection of pressurized drilling fluid into the open borehole, or to the pressure exerted by the regional stresses). Therefore, when interpreting statistics on the presence of open fractures in a fracture dataset, only general trends were considered.

Measurements of fracture apertures were seldom possible in shale outcrops due to surficial and shallow subsurface processes such as frost weathering and fracture filling with surficial materials, but it was quite often possible in well logs. In shallow wells, fracture aperture is directly measurable on acoustic televiewer (ATV) images (with a precision of around 1 mm), as open fractures generally display low amplitudes and high travel times (Davatzes and Hickman 2010). As closed/cemented fractures rarely produce geometric irregularities on the borehole wall, optical logs were also used to facilitate their identification in shallow wells. In deep shale gas wells, the aperture can only be observed indirectly using FMI data through resistivity contrasts. Since open fractures are filled with conductive fluids (brines or drilling mud), they display more conductive signatures than quartz- or calcite-cemented (healed) fractures. Resistive healed fractures also display a “halo effect” caused by the resistivity contrast between the filling and the host rock, which helps their identification (Thompson 2009).

Fracture apertures, estimated from shallow (ATV) and deep (FMI) well logs, are here called “apparent apertures” due to the sparsely distributed measurements that were available and because of the limitations of the methods (listed in Appendix 1). When comparing shallow ATV and deep FMI datasets, apparent apertures are markedly higher in the shallow aquifer (at least more than three orders of magnitude higher than in the deep shale gas wells). However, the magnitude of this difference must be interpreted with caution as the results were derived from two different estimation methods that both have important limitations (also listed in Appendix 1). In FMI logs, fracture apertures are approximately one order of magnitude higher in the lower portion of the IZ than in the deep reservoir. Fracture aperture estimates from FMI logs were available for both F1 and F3 fractures and there was no significant difference in aperture values when comparing these two fracture sets.

Finally, open and closed fracture densities were calculated along the wells using a counting window. The fracture densities were then normalized by the window length, so as to be expressed as a number of fractures per distance unit (one meter). More details on this approach are provided in Ladevèze *et al.* (2018).

3.2.3 Fracture porosity and permeability

Hydraulic properties related to open fractures (fracture porosity and permeability) within the IZ are critical when investigating potential upward fluid migration. However, a quantitative estimation of the hydraulic properties of the fractures is beyond the scope of this paper. The aim of this section is to assess semi-quantitatively the contribution of fractures to groundwater flow throughout the sedimentary succession, combining the conceptual model of the fracture pattern with available data inferred from well logs. Hydraulic property values were estimated using the existing datasets from the shallow aquifer (0-60 m within bedrock), the lower portion of the IZ (vertical well between 550 and 2000 m) and the reservoir (horizontal well).

The siltstone interbeds are mostly concentrated in the upper part of the Lorraine Group (see section 2.1) and because the focus of this study is on upward migration from the deep reservoir, the hydraulic properties of the siltstone units are not discussed here. Hydraulic properties for the IZ were thus estimated according to the REV of the shale units (Fig. 3c). To obtain representative values for hydraulic properties, the proportion of open fractures in each set and the median values of fracture spacing provided in Ladevèze *et al.* (2018) were used. Median values were preferred over their mean as the fracture spacing distributions exhibit a few extreme values. In addition, as no precise estimates of the fracture length are available (see section 2.2), the assumption was made that fractures crosscut the REV throughout its length (15 m). As a consequence, results obtained with this approach could be considered as an upper bound for realistic hydraulic property estimates.While the same fracture network (F1, F2 F3 and bedding plane fracture sets) was assumed to be present throughout the sedimentary succession, its geometric properties, found using mainly datasets from the shallow and deep intervals, can also be considered valid for the intermediate zone (Ladevèze *et al.* 2018). However, when considering hydraulic properties, two additional parameters must be taken into account: the variations in proportion of open fractures and the variations in fracture apertures. Three assumptions are proposed here to assess the hydraulic properties of the IZ based on the shallow and deep datasets. First, F1 fractures are considered as the dominant fracture set in the IZ (based on results of the well log analysis showing that open fractures in the deep interval belong mainly to this set). Second, the proportion of open F1 fractures observed in the reservoir is considered as an upper limit for the proportion of open F1 fractures in the lower portion of the IZ. These two assumptions are reasonable given that 1) the permeability anisotropy is stress dependent (Barton *et al.* 1995; Ferrill *et al.* 1999), 2) according to the *in situ* stress conditions in the SLP (Konstantinovskaya *et al.* 2012) (present-day maximum horizontal stress -S_{Hmax}- is oriented NE-SW), fractures that are aligned with the S_{Hmax} are more likely to be open (here, the NE striking F1 fractures, which is consistent with field observations in the reservoir when neglecting the small proportions of open F2 and F3 fractures) and 3) an increase in the magnitude of S_{Hmax} with depth is likely to open a higher proportion of fractures that are parallel with this stress orientation (here, the proportion of open F1 fractures is likely to increase with depth in the IZ and reservoir). Finally, the third assumption is that apertures estimated in the shallow aquifer can be used as proxies to estimate an upper bound for hydraulic properties of the upper portion of the IZ. In fact, the fracture apertures in the upper part of the IZ should be smaller than those from the shallow aquifers because processes such as uplift, decompaction and erosion may likely enhance the aperture of F1 fractures in the shallow interval. The degree of overestimation is, however, unknown.

The fracture porosity of the shale units within the Saint-Édouard area were estimated in shallow aquifers and at depth using Eqn (1):

$$\theta = \frac{\sum_{i=1}^{N} n_i b_i}{L} \qquad (1)$$

with $$n_i = \frac{L}{s_i} \qquad (2)$$

In Eqn (1), θ is the fracture porosity; i the fracture set (F1, F2, F3 or BPF); n_i the number of open fractures from set i; b_i is the aperture of the fractures from set i. and L is the length of the REV (15 m). In Eqn (2), s_i is the median spacing for fractures from set i.

Since very few F3 fracture spacing measurements were available from outcrops, data from the horizontal section of deep wells were used for the median spacing of F3 (as proposed in Ladevèze *et al.* (2018)). This value represents again an upper bound as these structures are likely to be more sparsely distributed in the IZ and shallow aquifer than in the reservoir. For the porosity estimates in the shallow aquifers, fractures from sets F1, F2 and F3 were considered open; in the IZ and in the reservoir, only F1 fractures were considered open.

Direct estimates of the hydraulic conductivity (*K*) were obtained in 14 shallow bedrock wells of the Saint-Édouard area using slug tests (Ladevèze *et al.* 2016). No direct measurement of *K* below 150 m from the surface was available in the study area. Drill-stem tests could not be performed in wells A, B and C due to the low permeability of the rock. Thus, the relationship between fracture aperture and *K* of the cubic law was used (Snow 1968). This model considers laminar flow between two parallel plates. The cubic law is either used to estimate *K* of a fracture using its aperture or to obtain its aperture (“hydraulic aperture”) using a known *K* value (generally field-based). This relationship can also be extended to estimate the hydraulic conductivity of a fracture system by considering regular sets of parallel fractures (Bear 1993). This concept is consistent with the fracture network presented in Figure 3 (Fig. 3c) when only considering open F1 fractures. The relationship takes the form of Eqn (3). The use of permeability (*k)* was preferred over hydraulic conductivity (*K*) at depth because the presence of a multiphase fluid flow system (with oil/gas and brines) makes the use of *K* less relevant. The parameter *k* is only a function of the medium (contrary to *K* that is a specific application of *k* to fresh water), which is thus more appropriate in this case. The *k* values were calculated using Eqn (4).

$$K = \theta \frac{b^2 \rho g}{12\mu} \tag{3}$$

and $$k = \frac{K\mu}{\rho g} \tag{4}$$

In Eqn (3), b is the aperture (in meters), θ is the fracture porosity (see Eqn 1), ρ is the fluid density in kg/m^3, μ is the dynamic viscosity in Pa.s and g is the gravitational acceleration (9.81 m/s^2). For comparison with available literature values on deep formations, *K* values available for the shallow interval were converted into permeability (*k*) using Eqn (3) and the thermo-physical properties of water. These properties were estimated using water temperatures at depth according to the mean geothermal gradient proposed in Bédard *et al.* (2014) for the SLP (23.0°C/km).

3.3 Characterization of fault zones

3.3.1 General approach

A fault zone is generally made up of a fault core surrounded by a damage zone, each of these structures being either a barrier to, or a conduit for, fluid flow (Caine *et al.* 1996; Bense and Person 2006; Bense *et al.* 2013). Fault zones affecting siliciclastic rocks thus generally display permeability anisotropy (Odling *et al.* 2004). Based on available field datasets, the potential contribution to fluid flow circulation of the core and damage zones was examined in this study. It must be emphasized that here only the natural conditions are studied based on existing and available data. However, fault behaviour can be modified depending on present-day stress change and pore-pressure increase related to fluid injection operations during hydraulic fracturing. If pore pressure increases, effective stresses decrease and the fault zone, which could have been sealed before these operations, can become critically stressed and reactivated (e.g, induced seismicity), thereby potentially facilitating fluid migration along this fault. The topic of fault behavior in a context of fluid injection operations is not addressed here.

Since no deep hydraulic tests were performed in the study area, the scope of this section is thus to provide insights into how the available data (borehole data, seismic data, and core analysis data such as the clay content) can help understand the fault zone behavior and whether the fault zones could facilitate upward fluid circulation through the sedimentary succession.

To analyse the control exerted by fault zones on groundwater flow dynamics, an integrated interpretation based on the existing datasets and previous studies of faults in the SLP was done. First, it must be noted that if a fault zone were to correspond to a flow pathway, its architecture would affect the fluid travel time. Therefore, architecture of the fault zones were analysed using the available structural cross-section in the study area (Lavoie *et al.* 2016). For this work, we follow the generally accepted hypothesis that fault planes that are aligned with the maximum horizontal stress (S_{Hmax}) are critically stressed (Barton *et al.* 1995). This hypothesis implies that faults that are mechanically alive are hydraulically alive and faults that are mechanically dead are hydraulically dead (Zoback 2010). The orientation of fault planes versus S_{Hmax} was also examined. Then existing evidence of fault sealing in the SLP were integrated into the analysis. Finally, specific analyses were made on existing datasets from thrusts and normal faults of the area (see section 3.3.2).

The key parameters of the two fault types present in the study area, which could impact fluid migration and that were investigated in this study, are summarized in Table 2. These characteristics should be examined and taken into consideration in assessment studies investigating potential upward migration.

Table 2 Summary of fault characteristics within the intermediate zone (IZ) that may enhance or limit upward fluid migration.

Fault characteristics that must be examined	**Enhance fluid migration**	**Limit fluid migration**
Open fractures in the vicinity of faults	Presence	Absence or open fractures parallel to one another (limited interconnection)
Lithologies	Faulting through high *K* rock	Faulting through low *K* rocks
Fault plane properties	Presence of some higher *K* units in the IZ	Dominance of low *K* materials
Fault dips	Steep dips and thus shorter pathways	Shallow dips and thus longer pathways
Fault orientation with respect to maximum principal stresses and its magnitude	Fault planes aligned with SH_{max} may be critically stressed	Fault planes orthogonal to SH_{max} are likely not critically stressed

3.3.2 Specific analyses

Core and log data were analysed to assess the impact of clay shearing on the hydraulic behavior of thrust faults. The shearing in clay-rich units (such as the shale-dominated succession of this area) is indeed known to form clay gouge in fault planes (Weber *et al.* 1978; Lehner and Pilaar 1997; Sperrevik *et al.* 2000), which is generally considered a barrier to fluid flow (Yielding *et al.* 1997; Freeman *et al.* 1998). The presence and characteristics of fractures in the vicinity of thrust faults was also documented and discussed here.

In addition, the fault core properties of a normal fault in the area (the Rivière Jacques-Cartier fault zone) were assessed using the Shale Gouge Ratio (SGR) (Yielding *et al.* 1997; Freeman *et al.* 1998). This widely used method is based on the estimation of the percentage of shale that has slipped past a certain point along a fault. The latter is then used to estimate the fault seal capacity. For comparison purposes, the empirical relationship of Sperrevik *et al.* (2002) was also used to estimate the fault core properties. This relationship was developed to describe the observed correlation between clay content and permeability (k, in mD) at the scale of fault core samples (Manzocchi *et al.* 1999; Sperrevik *et al.* 2002). This relationship also takes into account compaction and diagenesis effects, which strongly impact rock porosity and permeability and is particularly relevant for the study area. The reliability of this relationship was successfully tested in a comparable geological context (Bense and Van Balen 2004). Details are provided in Appendix 2. Fault seal analysis has been the focus of extensive recent studies (eg., Bense and Person, 2006) and the SGR method is only one of them. This approach has been selected for the present study because 1) the Sperrevik *et al.* (2002) method is based on field data from a comparable field geological context to the sedimentary succession of the SLP, 2) this approach takes into account the rock burial depth, which is a key parameter for rock permeability in the SLP and 3) it is also consistent with the approach successfully tested by Konstatinovskaya *et al.* (2012) using SGR in the SLP.

4 Results

4.1 Hydraulic characterization of the fracture network

4.1.1 Open fracture properties

General trends and observations related to fracture apertures in the present dataset are as follow: 1) high proportions of open features were identified in the shallow aquifer in all fracture sets (37%, 91% and 50% of the F1, F2 and F3 fractures, respectively) (Fig. 4a); 2) open bedding-parallel fractures (BPF) were only observed in shallow wells (Fig. 4a); 3) in the deep reservoir, a higher proportion of open F1 fractures was encountered in the horizontal legs drilled in the Utica Shale, compared with the F2 and F3 sets (21% of open F1 fracture versus 2% for F2 and F3 fractures) (Fig. 4d); 4) this higher proportion of open F1 fractures at depth was not observed in the vertical wells drilled through the Utica Shale (Fig. 4c and d) nor in the IZ, but this is very likely attributable to the fact that the high-angle fractures are significantly under-sampled in vertical wells; 5) while approximately the same number of open fractures was identified in the IZ and gas reservoir using the three vertical wells, this number was obtained for very different cumulative well lengths: the segments logged in the reservoir were typically more than four times shorter than in the IZ. Much more fractures were identified in the more brittle Utica Shale (Fig. 4b and c), in agreement with previous observations by Ladevèze *et al.* (2018) considering all fractures (see for instance Fig. 3). Therefore, lithology seemingly controls the number of open fractures.

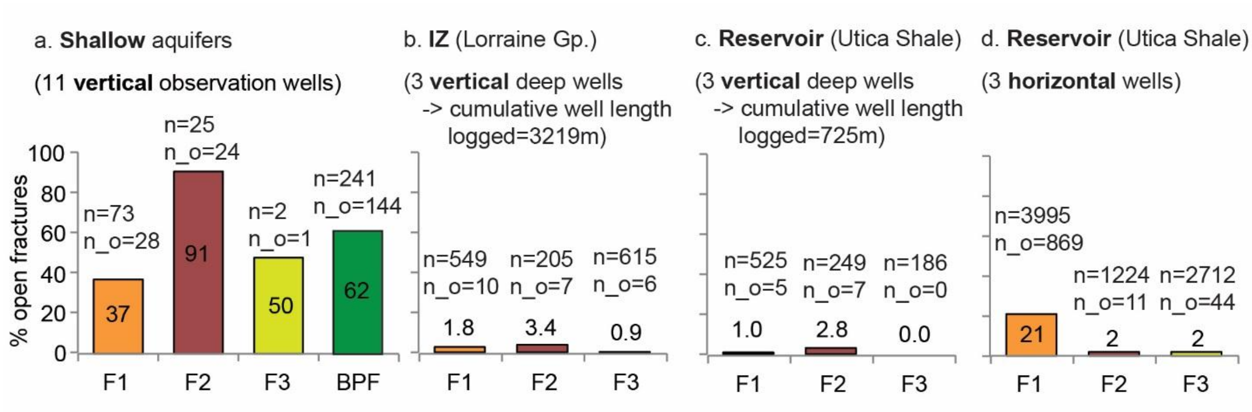

Fig. 4 Percentage of open fractures from the total fracture population for the F1, F2, F3 and BPF sets according to the data source; n: total number of fractures; n_o: number of open fractures; F1, F2 and F3: three high-angle fracture sets; IZ: Intermediate zone; BPF: bedding-parallel fractures; Gp.: Group.

As mentioned earlier, estimated apertures may be considered slightly overestimated since fracture apertures are likely to be enhanced by drilling operations, especially in finely layered rocks such as shales. This is particularly the case in the shallow aquifer where the rock decompaction further enhances this process. For this reason, some extreme aperture values (typically >10 mm) measured at shallow depth using acoustic televiewer data (Crow and Ladevèze 2015) were excluded from the analysis. Moreover, deep fracture apertures can also be slightly overestimated when using FMI because of the limitations of the aperture estimation method (Davatzes and Hickman 2010). As a consequence, the fracture aperture values presented in Table 3 likely represent an upper limit for realistic values in the study area.

Table 3 Available estimates for fracture apertures for the shallow and deep intervals.

	Shallow wells	Deep well B High-angle open fractures

	Open bedding-parallel fractures (BPF)	High-angle open fractures (F1, F2, F3)	IZ - Lorraine Group (vertical well: 560 to 2000 m)	Reservoir – Utica Shale (horizontal well)
Apparent apertures (mm)				
Median	2.0	3.0	0.048	0.0038
Min / Max:	1.0 / 8.0	1.0 / 8.0	0.019 / 0.094	0.0013 / 0.055
No. of estimations	13	13	12	16

Shallow observation wells show an exponential decreasing trend of the open fracture density within the upper 60 m of bedrock, with most of the open fractures being located in the first 30 m (Fig. 5b, same trend for the two types of open features). There is no clear trend for the density distribution of closed fractures with depth for the shallow observation wells (Fig. 5c). The dataset for deep wells did not show any specific trend in the distribution of open fractures within the sedimentary succession.

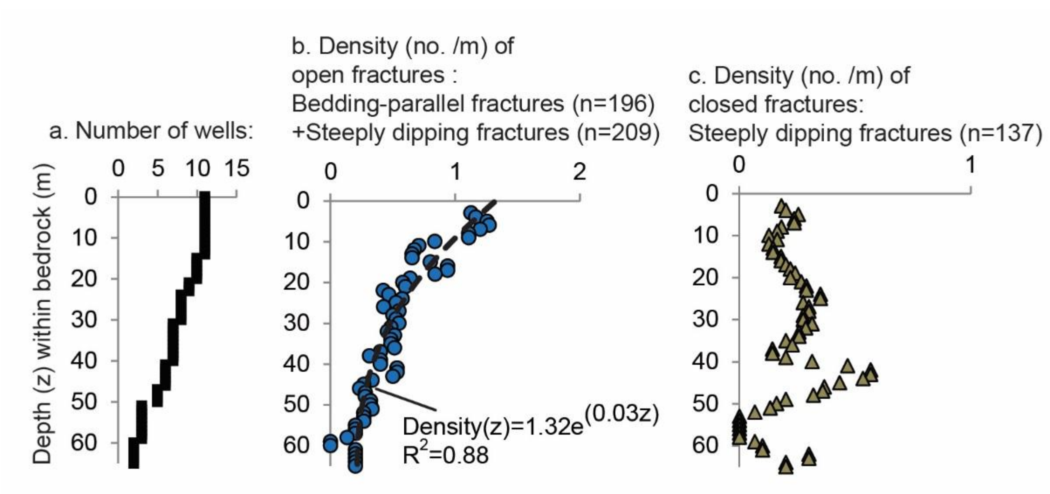

Fig. 5 Fracture density variations with depth within the bedrock in shallow wells. Data from 11 observation wells were combined. Fracture densities were calculated using a 5 m window length every 1 m. The number of wells according to the depth within the bedrock was used to normal-

ize fracture densities.

4.1.2 Assessment of the hydraulic properties throughout the succession

Fracture porosities, *K* and *k* values calculated for the shallow aquifer are presented in Figure 6 according to the depth at which aperture measurements are available (values presented in Appendix 3). The median fracture spacing values considered for the estimation of the number of open fractures in the REV are respectively 0.2, 2.51, 0.11 and 0.17 m for the F1, F2, F3 and BPF fracture sets. Fracture aperture values used to calculate porosity come from Table 3. As the rock mass of the shallow aquifer has open fractures that locally display some large apertures, the fracture network significantly contributes to the total porosity of the rock mass (up to approximately 8%). Hydraulic conductivities ranging from 2.3×10^{-9} to 1.1×10^{-5} m/s (with a median of 6×10^{-7} m/s) were obtained from hydraulic tests performed in 11 shallow observation wells (less than 145 m deep), all open to bedrock (Ladevèze *et al.* 2016). Higher *K* values were obtained in wells located in the autochthonous domain, with a marked correlation associated with the presence of siltstone interbeds. Wells in the parautochthonous domain intersect shale units that are highly folded and faulted and display lower *K* values. These values suggest the presence of significant fluid flow circulation at shallow depth in the fractured shale-dominated aquifer, mainly through open BPF that are connected to open sub-vertical fractures. Figure 6 also presents fracture porosities, *K* and *k* values calculated for the IZ and reservoir with Eqns 3 and 4 using the fracture aperture estimates provided in Table 3 (values available in Appendix 3). The median fracture spacing value considered for the estimation of the number of open F1 fractures in the REV is 0.14 m (measured in horizontal sections of deep wells, see Ladevèze *et al.* (2018) for more details).

Contrary to those in the shallow units, deeper open fractures only slightly contribute to the total porosity. Pores of the rock matrix are then the most significant contributors to total porosity, as the latter was reported having a median value of 3.3% for the Lorraine Group and the Utica Shale based on laboratory and log analyses on core samples (BAPE 2010; Nowamooz *et al.* 2013; Séjourné *et al.* 2013; Séjourné 2015). Extremely low values of K and k for the deep fracture network were thus obtained using the cubic law and the apertures estimated in both the lower portion of the IZ and in the reservoir. Nonetheless, these geometric mean k values (10^{-18} to 10^{-24} m^2) are within the range of matrix permeabilities proposed in the literature for the deep units of the Lorraine Group and Utica Shale: geometric mean values around 10^{-20} m^2, with extreme values ranging from 10^{-16} to 10^{-27} m^2 (BAPE 2010; Séjourné *et al.* 2013). When considering the fracture apertures estimated in the shallow aquifer for F1 fractures, values of k around 10^{-13} m^2 are obtained, which are close to the upper limit of the range reported for the deeper units.

No clear trend with depth of the hydraulic properties was identified in the lower portion of the IZ and in the reservoir (Fig. 6). However, when comparing the values estimated in each of the geological intervals (shallow aquifer, upper portion and lower portion of the IZ and reservoir), there is a global decreasing trend for these values with depth. As such, only limited fluid circulation can be envisioned in the lower portion of the IZ and in the reservoir.

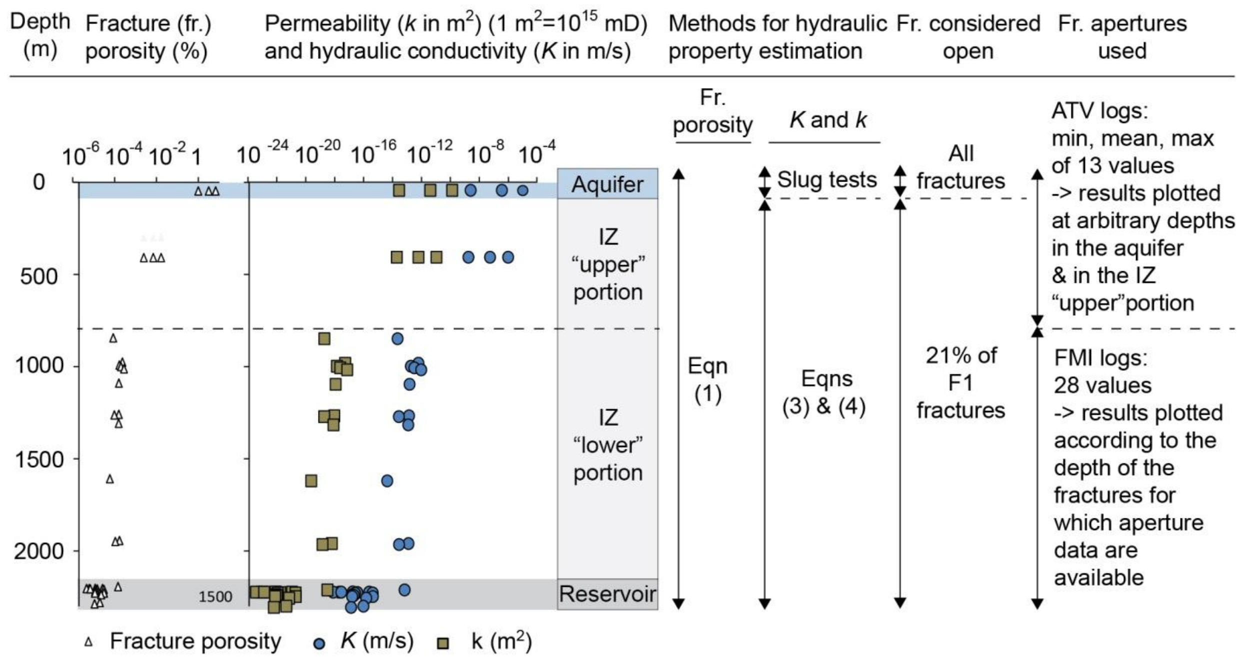

Fig. 6 Variation with depth of the estimated fracture porosities, hydraulic conductivity (*K)* and corresponding permeabilities (*k). K* values from slug tests (field data) were initially presented in Ladevèze et al., 2016. ATV: Acoustic Televiewer; FMI: Formation Micro Imager; IZ: Intermediate Zone. Numerical values are presented in Appendix 3.

4.2 Hydraulic characterization of fault zones

4.2.1 Fault zone architecture

The autochthonous domain of the SLP hosts some isolated and steeply dipping normal faults, such as the Rivière Jacques-Cartier fault (Fig. 1). Their steep dips combined with the overall thinning of the sedimentary succession and the shallowing of the platform towards the northwest would provide the shortest and most direct pathways between the Utica Shale and fresh water aquifers. This geometry contrasts with the parautochthonous and allochthonous domains to the southeast, where shallow-dipping regional thrust faults propagate from southeast to northwest

(Fig. 1), often displaying an imbricated fan geometry (St-Julien *et al.* 1983; Séjourné *et al.* 2003; Castonguay *et al.* 2006).

Therefore, potential pathways in thrust faults of the study area would have to develop over much longer distances than in normal faults, not only because the Utica Shale is much deeper than in the northern part of the study area, but also due to the much more complex geometry associated to the thrust faults.

4.2.2 Thrust fault zone

Fine-grained rocks were observed in fault planes identified in a few core samples (**Erreur ! Source du renvoi introuvable.**) from shallow wells; they are here called “gouge”, as proposed by Sibson (1977). Gouge was also observed in the thrust fault planes of the parautochthonous domain on optical logs of a few shallow observation wells. The presence of this gouge may have caused the sealing of the fault core, which would thus constitute a barrier to fluid flow. Heat-pulse flowmeter tests performed in several shallow observation wells (Crow and Ladevèze 2015) confirmed that little to no flow occur in the presence of these thrust fault planes. This is also consistent with the low hydraulic conductivity values calculated in shallow wells of this area, which displays significant faulting/folding evidence that is characteristic of the parautochthonous domain (Ladevèze *et al.* 2016). Nonetheless, the presence of a few open fractures was also noted in some of these logs and can probably explain the presence of local shallow fluid flow circulation (see for instance the slight variation in the fluid conductivity log in the vicinity of an open fracture in **Erreur ! Source du renvoi introuvable.**).

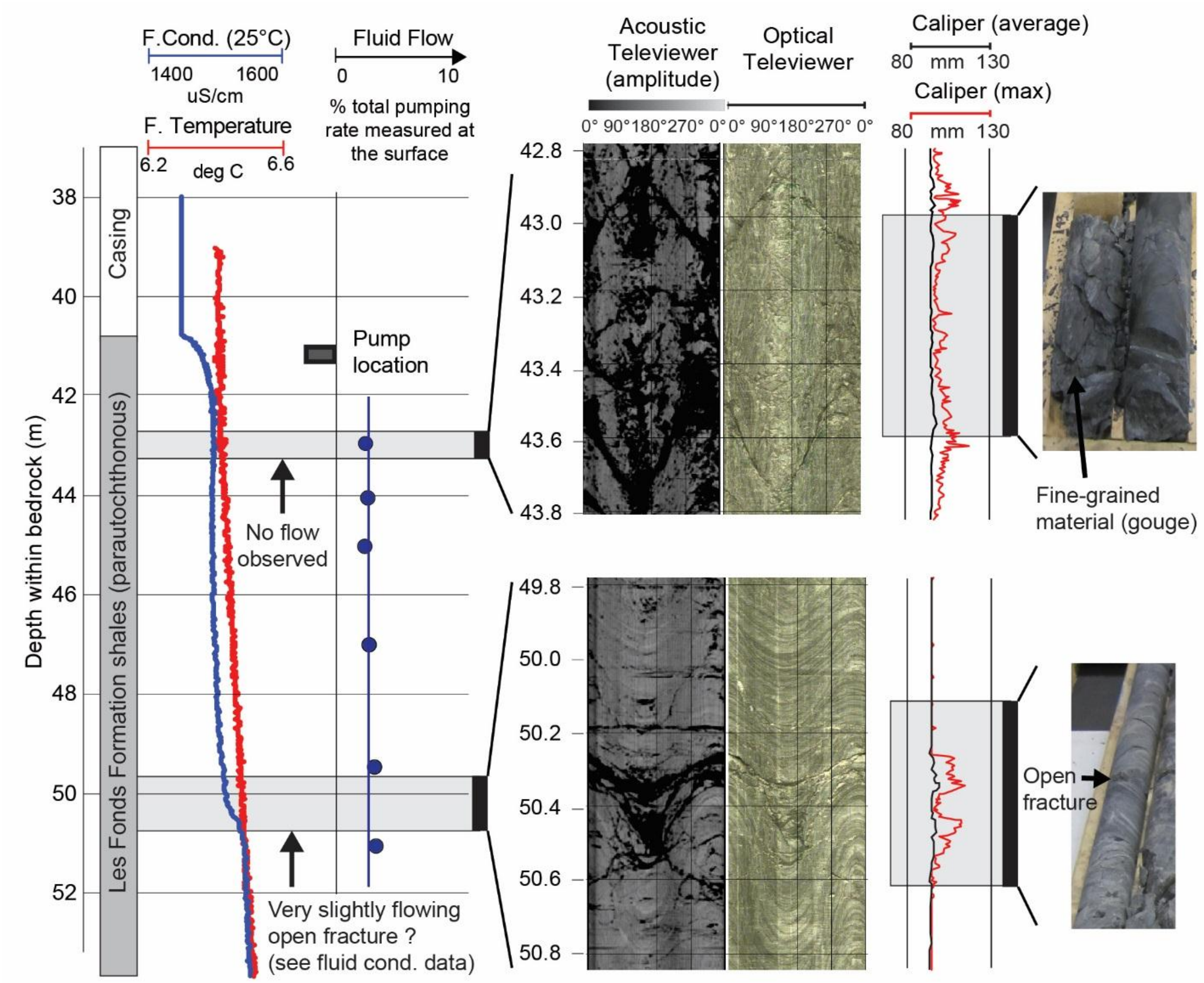

Fig. 7 Examples of results obtained from borehole geophysical logging (Crow and Ladevèze 2015) performed in a 50 m observation well drilled in the parautochthonous domain within the thrust sheet domain, showing intervals with noticeable faulting and folding, along with open fractures.

Data from deep shale gas well logs indicate that open fracture densities associated with thrust planes were higher in the vicinity of the Appalachian structural front (see Appendix 4 showing higher values for well A). This finding is in agreement with previous observations when considering fractures without considering their aperture (Séjourné 2015; Ladevèze *et al.* 2018). Nonetheless, open fracture density values obtained in the deep shale gas wells remain significantly lower than those calculated in the shallow observation wells (see values in Fig. 5).

These preliminary observations suggest that there is a possible correlation between open fracture density and the presence of faults. To confirm this potential relationship, a more detailed comparison of open fracture density variation with fault proximity was undertaken at the borehole scale using FMI data from the horizontal leg of well A, where a fault zone can be observed. In well A, the fault zone is within the Utica Shale and consists of a highly fractured damage zone that surrounds two fault planes that are dipping toward the NW at about 25° (the two planes are closely spaced, so to simplify the analysis, only one plane is hereafter considered) (Ladevèze *et al.* 2018). In this section of well A, almost all the open fractures have the same orientation as F1 fractures (95 % of the open fractures in the horizontal portion of well A).

The open fracture density globally decreases with increasing perpendicular distance from the fault zone (**Erreur ! Source du renvoi introuvable.**). The open fracture distribution is clearly not continuous along the horizontal portion of the well, but rather show clusters. Figure 8b shows that in well A, three fracture clusters are separated by distances of approximately 80 to 135 m. As proposed in Ladevèze *et al.* (2018), F1 fractures are likely concentrated in corridors, although this pattern remains to be confirmed. Therefore, this suggests that these open fractures probably belong to the F1 set, although the possibility of the existence of a new fracture set associated with these fault zones cannot currently be dismissed.

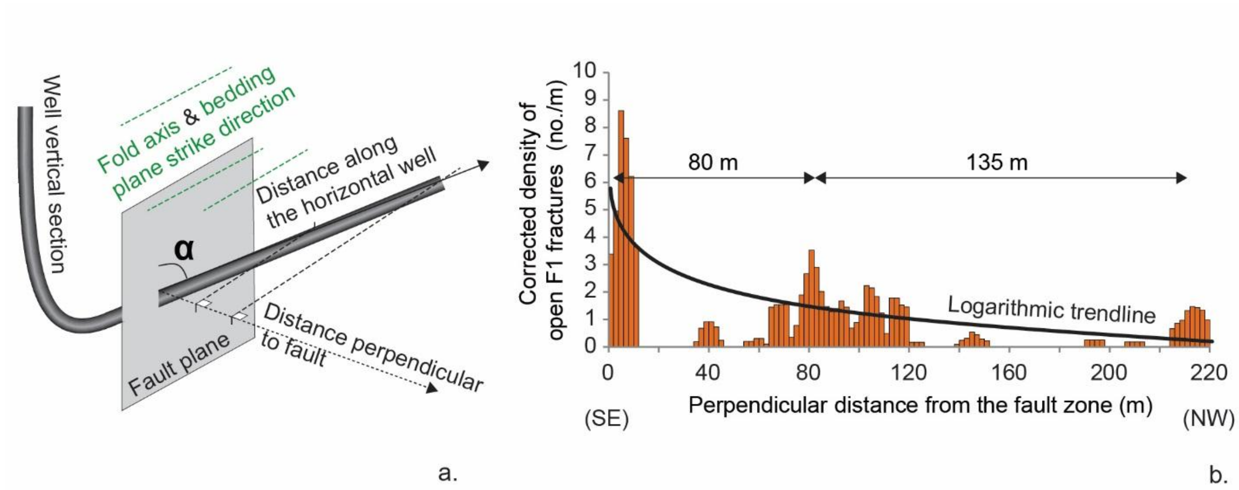

Fig. 8 Open fracture density variation in the vicinity of a fault plane in the horizontal section of well A: **a.** conceptual diagram illustrating the difference between the distance perpendicular to the fault and the distance along the horizontal section of the well (used to estimate the possible relationship between fracture density and fault proximity). The angle α represents the angle between the fault plane and the borehole direction; **b.** density variations of open F1 fractures with respect to the distance from a fault zone in the horizontal portion of well A. Fracture densities were corrected for sampling bias using the Terzaghi (1965) method.

4.2.3 Normal fault zone

In the SLP, the high angle (near vertical) NE-SW faults (normal faults) oblique to S_{Hmax} are more likely to be reactivated (Konstantinovskaya *et al.* 2012). Therefore, these normal faults are likely critically stressed and potentially hydraulically active. However, this hypothesis would need to be addressed more in details, but a thorough study of the hydro-mechanical attributes of the Rivière Jacques-Cartier fault to further assess the impact of the fault reactivation on its hydraulic properties is beyond the scope of the paper.

To the south-west of the study area, observations from at least two deep wells have shown that gouge forms in normal faults of the SLP (wells A027 and A125 in the Bécancour area; see Séjourné *et al.*, 2013). Clay-rich shales were also suspected to have been displaced along the Rivière Jacques-Cartier normal fault. Because the stratigraphic units that are cut by normal faults (shales from the Lorraine Group) contain a significant proportion of clay, the term "clay gouge" (Vrolijk *et al.* 2016) is used hereafter.

In this area, the calculated SGR values decrease progressively with increasing depth (Fig. **Erreur ! Source du renvoi introuvable.**) since the volume of shale (V_{sh}) also decreases progressively with increasing depth in the sedimentary succession (shale-dominated to carbonate-dominated units). SGR values over 20% (interpreted as sealed structures according to (Yielding *et al.* 1997)) were calculated for the segments of the normal fault above the Utica Shale reservoir (Fig. **Erreur ! Source du renvoi introuvable.**); this value suggests the presence of clay gouge in these segments and, hence, a sealing behavior. These preliminary results are in agreement with a similar analysis carried out for the Yamaska fault to the south-west of the study area (Konstantinovskaya *et al.* 2014b). Moreover, in both regions, lower SGR values were found in carbonate-dominated units below the Utica Shale, suggesting a slightly more permeable medium.

With the Sperrevik *et al.* (2002) equation, k values range approximately from 10^{-21} to 10^{-24} m^2 and 10^{-24} to 10^{-26} m^2 respectively for the core of theoretical Fault 1 and 2 in Figure. **Erreur ! Source du renvoi introuvable.**. These values are either similar to or lower than those obtained for the fracture network at depth using the cubic law relationship (see Fig. 6). Although not considered precise, these semi-quantitative estimates confirm that permeability values of the normal fault core is likely extremely low. These results also advocate for significant sealing behavior of the fault core in the IZ, impeding flow across it. Moreover, this analysis highlights the crucial need for field data, including *in situ* permeability tests or pressure gradient estimations across a fault zone, to better calibrate these empirical relations and to more accurately determine the hydraulic behavior of the fault gouge.

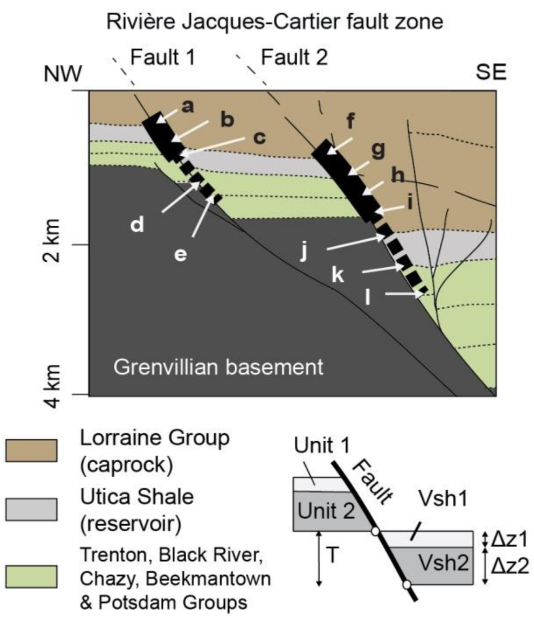

Location	SGR (%)	k (m^2)	K (m/s)
Fault 1			
a	44	4.4×10^{-24}	6.0×10^{-17}
b	21	2.4×10^{-24}	3.2×10^{-17}
c	12	4.6×10^{-22}	6.2×10^{-15}
d	14	6.4×10^{-21}	8.7×10^{-14}
e	13	1.6×10^{-21}	1.2×10^{-14}
Fault 2			
f	44	1.3×10^{-24}	1.7×10^{-17}
g	37	2.4×10^{-25}	3.3×10^{-18}
h	22	7.1×10^{-26}	9.6×10^{-19}
i	18	2.1×10^{-26}	2.8×10^{-19}
j	19	1.7×10^{-24}	2.3×10^{-17}
k	15	5.3×10^{-24}	7.2×10^{-17}
l	5	2.0×10^{-26}	2.7×10^{-19}

SGR > 20% $K_{Gouge} >>> K_{shale\ matrix}$

SGR < 20% K_{Gouge} = or > $K_{shale\ matrix}$

Fig. 9 Cross-section of the Rivière Jacques-Cartier fault system (see location in Fig. 1) used for the Shale Gouge Ratio (SGR), permeability (k) (expressed in m^2; 1 m^2=10^{15} mD) and hydraulic conductivity (K) calculations along the fault planes of the Rivière Jacques-Cartier fault. T: fault true displacement; Δz: thicknesses of the stratigraphic units; V_{sh}: volume of shale.

5 Discussion

5.1 Hydraulic behavior of open fractures

Based on the open fracture distribution in the shallow fractured rock aquifer, IZ and reservoir, two hydrogeological domains were defined. The first corresponds to the shallowest portion of the bedrock where most of the flow is concentrated (active flow zone). The second hydrogeological domain corresponds to the IZ and reservoir (deep intervals) where very little flow takes place. Most of the open fractures are concentrated in the upper 30 to 60 m of bedrock, although some open fractures were also locally observed down to 145 m in the deepest observation well of the study area (Crow and Ladevèze 2015). However, as this well displays particularly low *K* values ($\pm 10^{-9}$ m/s) compared to the other observation wells, these fractures seemed to be nearly hydraulically inactive (Ladevèze *et al.* 2016). Thus, an arbitrary limit of 60 m within bedrock is proposed here to delimit the two hydrogeological domains, but it must be kept in mind that this boundary is gradual and could certainly be spatially variable. Nonetheless, geochemical profiles performed in four of the shallow observation wells (drilled between 15 to 145 m within the shallow fractured rock aquifer) indicated that water types changed from $CaHCO_3$ or $NaHCO_3$ (corresponding to relatively recent water) in the upper part of the wells, to NaCl at the bottom (corresponding to evolved water with much longer residence time) (Bordeleau *et al.* 2018b), thereby providing additional evidence for the lower limit of the shallow groundwater active zone.

5.1.1 In the shallow rock aquifer

In the shallow rock aquifer (0-60 m within bedrock), there is a high proportion of open fractures, both sub-vertical and sub-horizontal, which have apertures larger than 1 mm. This high proportion of “large” open fractures plays a significant role for groundwater circulation, especially where open BPF are interconnected with sub-vertical open fractures. The decreasing density of open BPF within the first 60 m is likely to be related to the increase of the stress normal to BPF planes as a consequence of the increase of the overburden stress with depth. The degree of connectivity of open fractures, and thus fluid circulation, is thus limited as depth increases.

The NW striking F2 fracture set seems preferentially open (91% of F2 fractures). The preferential opening of the F2 set would, however, need confirmation as there is a high risk of error in classifying fracture orientations using shallow well log data and their number was limited (25). The other facture sets also display significant proportions of open fractures (37% of F1 fractures and 50% of F3 fractures). Thus, in shallow wells, the orientation is not a critical factor for fracture opening as total stresses tend to be equal at shallow depth. This finding contrasts with the statement that open fractures (and thus the anisotropic permeability tensor) should be preferentially oriented parallel to the orientation of the present-day maximum horizontal stress (S_{Hmax}) in shallow aquifers (Mortimer *et al.* 2011). In fact, S_{Hmax} is oriented NE-SW in this region (Konstantinovskaya *et al.* 2012), parallel to the orientation of the F1 fractures. The probable explanation is that previously closed fractures could have been re-opened under the influence of post-glacial surface processes. It is indeed recognized that episodes of glaciation and deglaciation can enhance the opening of pre-existing fractures at shallow depths (Wladis *et al.* 1997; Martini *et al.* 1998). These effects, combined with decompaction in a context of erosion and uplift, could likely explain the opening of fractures at shallow depths regardless of their orientation.

5.1.2 In the deep intervals (intermediate zone and reservoir)

The situation is different below this *circa* 60 m threshold, as most of the open fractures observed are sub-vertical, essentially belonging to the F1 fracture set. F1 fractures are parallel to the contemporary NE-SW orientation of S_{Hmax}, thereby in agreement with the theory proposed by Barton *et al.* (1995) stating that the contemporary *in situ* stress regime at depth should preferentially control the opening of fractures that are aligned with S_{Hmax}. It must also be noted that overpressured conditions were identified in the Utica Shale and at the base of the Lorraine Group (Morin 1991; BAPE 2010; Chatellier *et al.* 2013) could also be responsible for the presence of these open fractures. However, because the dissolution of fracture fillings may contribute to the presence of open fractures whatever their orientation (Laubach 2003; Laubach *et al.* 2004), the existence of open fractures from the F2 and F3 sets cannot be discarded. Nonetheless, few observations of such features were made in well logs. For this reason, it is concluded that the *in situ* stress regime is the dominant cause for fracture opening at depth.

Bedding-parallel fractures were not specifically observed in the available shale gas well logs, but were documented by a few authors in other shale gas plays (Rodrigues *et al.* 2009; Gale *et al.* 2015). Because of the overburden pressure on the sedimentary succession, the BPF should be closed at depth in spite of overpressured conditions documented in deep hydrocarbon exploration wells identified in the Utica Shale and at the base of the Lorraine Group. Hence, these structures are not considered conductive for fluid flow.

A fluid flow model of this study area should thus take into account the fact that the hydraulic conductivity (K) would likely be anisotropic, with a preferential orientation according to the F1 fracture strike. Moreover, as the fractures are rotated according to bedding plane orientations (Ladevèze *et al.* 2018), the K tensor should follow these bedding plane orientations, as proposed in the work of Borghi *et al.* (2015).

The proposed analysis of the contribution of open fractures to fluid circulation at depth was carried out using analytical solutions based on theoretical assumptions and limited available datasets of fracture apertures and open fracture distribution in rock mass. Therefore, the calculated values must be considered with caution. Also, the method based on the cubic law has been challenged for fractures displaying low aperture values (less than 0.004 mm, which is the case here when considering fracture apertures from the reservoir) (Witherspoon *et al.* 1980). Furthermore, these calculations are based on the assumption of a laminar flow between two parallel fracture planes. This assumption can lead to significant errors, as it is now documented that the geometry of the fracture wall significantly controls its hydraulic properties (Méheust and Schmittbuhl 2001; Berkowitz 2002) because it induces flow channeling within the fracture (Tsang and Neretnieks 1998; Berkowitz 2002). It was also demonstrated that depending on the hydraulic gradient orientation in the fracture, fracture wall roughness can both reduce or enhance fracture permeability estimates compared to parallel plates (Moreno *et al.* 1990). Despite the fact that flow channeling and wall roughness are not taken into account, the extremely low calculated K and k values advocate for very limited fluid flow circulation in the open fractures at depth.

F1 fractures (open and closed) were found to be pervasive throughout the sedimentary succession, but their vertical extent is unknown (Ladevèze *et al.* 2018). Nonetheless, the contribution of open F1 fractures, both to porosity and permeability, seems to be small (Fig. 6). Therefore, even if open fractures were identified at depth, their control on K is limited. In fact, natural open fractures can certainly enhance the K at depth (although obviously to a very limited extent), but the magnitude of this variation is unknown because no direct hydraulic tests are available in this region and uncertainty on the value of fracture apertures is likely large, which in turn strongly impacts permeability estimates when using the cubic law. Values of k presented in Fig. 6, although considered as upper limits, advocate for very limited fluid flow circulation in the open fracture network. Moreover, fracture apertures such as the mean and maximum values estimated in the shallow aquifer are very unlikely to exist below a few hundred meters. It is thus very likely that permeability values estimated for the lower portion of the IZ apply to most of the IZ, which also suggests very limited fluid circulation in the fracture network.

For this reason, open fractures can be regarded as features that can potentially increase K values locally, but further work should be carried out to quantify this increase (comparatively to the K of the shale matrix). This important issue was also pointed out in other shale gas plays such as the

Barnett Shale in Texas, where unhealed, potentially open fractures were also observed (Gale *et al.* 2007). However, some authors argue that they are merely closed and, as such, do not significantly affect the reservoir permeability (Bowker 2007).

5.2 Additional considerations regarding the potential for upward migration

5.2.1 Overpressure conditions

In a context of low water saturation within the Utica Shale, between 17.2 and 29.2 % (BAPE 2010; Séjourné 2015), the overpressure conditions should mostly be caused by high natural gas concentrations, which indicates that large-scale water circulation has not been occurring. Indeed, the existence of an overpressure regime in the reservoir combined with the presence of hydrocarbons may be interpreted as an indicator of the hydraulic seal capacity of the reservoir, according to the concepts described by Watts (1987); Ortoleva *et al.* (1995); Osborne and Swarbrick (1997). Thus, even if regional scale faults are present in the sedimentary succession, they do not appear to provide migration pathways between the deep gas reservoir and the shallow aquifer.

This sealing behavior is also in agreement with the differences in fluid pressure observed on each side of the Yamaska Fault in the SLP (in the Bécancour area, see Fig. 1 for its location) and mentioned by Konstantinovskaya *et al.* (2014b) and Tran Ngoc *et al.* (2014).This pressure unbalance is likely related to the absence of fluid circulation across this fault plane.

5.2.2 Contribution of siltstone interbeds to fluid circulation in the normal fault zone

In the shallow observation wells drilled in the Saint-Édouard area, the presence of siltstone interbeds was noted in the vicinity of the Rivière Jacques-Cartier Fault and was shown to be a major factor contributing to higher measured K values (Ladevèze *et al.* 2016). These siltstone interbeds were found to be more fractured than the shale units (represented in Fig. 3c and d), thus enhancing fluid circulation. In deeper horizons, siltstone beds, which are frequently present in the upper part of the IZ, should also have higher permeability values and could increase permeability when present in the vicinity of faults.

Also, the amount of clay-sized particles in siltstone is lower than in shales, thus limiting the potential for gouge to form as a result of friction in fault planes. Furthermore, when faulted, some siltstone beds are likely to be dragged into the fault core, thereby locally increasing their permeability compared to the shale host rock. Similar observations were made by Bense and Person (2006) in faulted sandstone/shale successions; they showed that the presence of sandstone interbeds dragged into the fault core is more likely to enhance flow along the fault plane than flow across the fault zone (Bense and Person 2006).

This is also consistent with the previously demonstrated fact that the pore fabric of more porous rocks such as sandstone in the vicinity of fault zones is modified, leading to permeability anisotropy in these zones with a maximum permeability tensor oriented in the direction of the fault plane (Farrell and Healy 2017). In addition to these porosity modifications, the presence of a fracture network in the fault core and damage zone is also likely to cause permeability anisotropy in fault zones affecting sandstones (Bossennec *et al.* 2018). The same phenomenon should also occur in fault zones comprising siltstone/shale successions, such as those of the Saint-Édouard area, especially in the upper units of the Lorraine Group in the Rivière Jacques-Cartier fault system (as opposed to the thrust fault area, where much lower siltstone content was found near the surface). However, the maximum depth where a significant content of siltstone interbeds can be found is currently unknown for the Saint-Édouard area. Therefore, the maximum depth at which siltstone can be dragged into the fault core is also unknown, but this should only occur in the upper part of the Lorraine Group units, where siltstones are dominant (up to 80% of siltstones). The dragging of siltstone strata into the fault core at shallow depths could thus help explain how groundwater containing brines was found in a few shallow observation wells close to the normal fault (Bordeleau *et al.* 2018b).

5.3 Conceptual models for deep circulation in fractures and fault zones

The objective of this study was not to precisely quantify the risk to shallow groundwater quality related to potential shale gas exploitation in the Saint-Édouard area, but to make a preliminary assessment of the potential for upward migration through the IZ based on commonly available field data. The topic of fault behavior in a context of hydraulic fracturing operations was not addressed here.

Figure 10 provides schematic diagrams summarizing the different structural features that potentially impact fluid flow in the Saint-Édouard area and that have been described in previous sections. Flow circulation in the IZ should be strongly controlled by the presence of open fractures that primarily strike to the NE (F1 fractures) in agreement with the present-day *in situ* maximum horizontal stress (S_{Hmax}), based on observations made in the reservoir and at the base of the IZ. As very few open fractures from the other sets could be observed at depth, the potential interconnection of open F1 fractures with other open fractures is likely severely limited. Consequently, the bedrock should be strongly anisotropic with respect to hydraulic conductivity (*K)* (Fig. 10a) and fluid flow circulation should also be very limited. At shallow depths (0 – 60 m within the rock aquifer), since most of the fractures in the different sets present a significant proportion of open fractures, the *K* tensor should only be weakly anisotropic. The presence of open bedding-parallel fractures that interconnect the high-angle fractures from the F1, F2 and F3 sets also contribute to much higher *K* values in the shallow rock aquifer compared to those in the IZ and the shale gas reservoir.

Based on existing data and observations, a combined conduit-barrier system with a sealed fault core was proposed for the conceptual models of the fault zones of the Saint-Édouard area (Fig. 10b). The core of both thrust and normal faults should be considered as a barrier to fluid flow. In contrast, the damage zone surrounding these fault cores could be more permeable than the rock matrix elsewhere. This could be the consequence of the presence of a larger density of open fractures, although mostly displaying the same orientation as F1 fractures (which is parallel to S_{Hmax}) in the case of the thrust fault system (Fig. 10c.2), or due to the presence of dragged siltstone beds within the core in the case of the normal fault system (Fig. 10c.1). Hence, deep flow (likely representing a relatively small quantity compared to water circulating in the active zone) should not cross the fault cores, but could eventually circulate upward over some distance into the fault damage zone, under the control of a sufficient hydraulic gradient, towards the more fractured shallow zone. It is also assumed that in the thrust fault zone, a small portion of the flow may also be able to pass through at different depths of the IZ, likely where sedimentary thrust slices are present. The current field datasets do not, however, allow the estimation of magnitudes for these potential local permeability enhancements. In fact, the latter should be further mitigated by the fact that the open fractures close to thrust faults are crosscut by closed or healed fractures at depth. Also, the presence of open fractures in the vicinity of the normal fault zone was not confirmed with direct field observations or data as no gas wells are present in this area. Nonetheless, upward fluid migration over a few hundred meters is strongly supported by geochemical results (Bordeleau *et al.* 2018b).The numerical modeling done by Janos *et al.* (2018) also indicated that upward fluid flow could indeed occur in the Rivière Jacques-Cartier fault zone if it did actually behave as a conduit-barrier system.

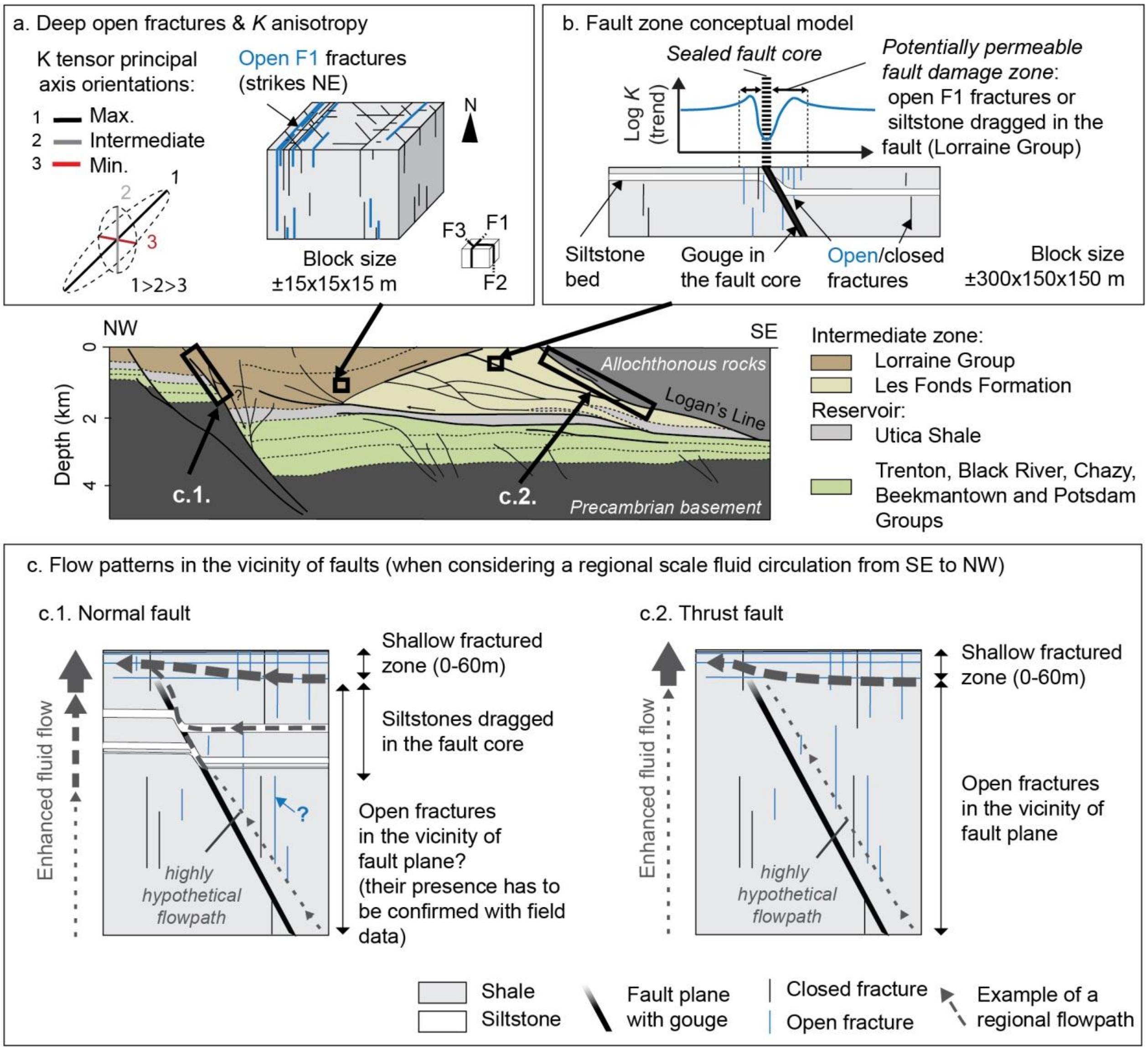

Fig. 10 Conceptual models summarizing potential groundwater flow patterns associated with fractures and faults: **a**. deep open fractures (intermediate zone and reservoir) and their impact on the hydraulic conductivity tensor at a metre scale (conceptual model of the fracture network: see Ladevèze *et al.* (2018)); **b**. potential *K* variations in the vicinity of faults and **c**. regional flow pattern in the vicinity of faults. These conceptual models are presented in their regional context using the cross-section shown in Fig. 1. In b. and c. the vertical extents of fracture planes are not to

scale.

These concepts and current field evidence do not support the existence of large-scale upward migrations from the reservoir towards fresh water aquifers in the Saint-Édouard area. Such pathways are thus considered highly hypothetical at best and are represented using dotted lines in Figures 10c.1 and 10c.2. Nonetheless, the current lack of field measurements of hydraulic properties in the vicinity of fault zones makes it impossible to reach unequivocal conclusions. The acquisition of additional field data, especially related to hydraulic properties and vertical extension of open fractures in the vicinity of these fault zones would be highly beneficial to validate and refine these models.

6 Conclusions

In the context of unconventional oil and gas exploration and exploitation, there is a need for a better understanding and representation of potential preferential flow pathways in hydrogeological models to assess the risk of contaminant migration from the stimulated oil or gas reservoir to shallow aquifers. While impact assessments must be data-driven, the intermediate zone located between shallow aquifers and the deep hydrocarbon reservoir is generally poorly documented. In this perspective, this paper provides key elements of a methodology that could be applied within the framework of a preliminary environmental study, aiming to ultimately assess risks of potable groundwater contamination related to deep industrial activities, where only limited datasets are currently available.

This contribution focused on determining whether the structural discontinuities affecting a given area of the St. Lawrence Platform (Quebec, eastern Canada) could constitute natural flow pathways between the Utica Shale unconventional reservoir and the shallow fresh water aquifers.

Several natural fracture sets and regional faults were known in this area (Lavoie *et al.* 2016; Ladevèze *et al.* 2018). However, their structural characteristics, as well as the possibility of upward flow circulation through them remained to be defined. It was concluded, based on findings from this research, that the existence of large-scale preferential flow pathways is not unequivocally ruled out but is deemed to be unlikely in the study area. In addition to more fieldwork needed to assess the hydraulic properties of the fault zones at depth, a detailed study of driving mechanisms should also be carried out so as to better define and eventually quantify the risk of upward fluid migration from a deep reservoir in the vicinity of faults.

Although the results and conclusions proposed here are truly meaningful only for a small portion of the St. Lawrence Platform of southern Quebec, the approach presented here outlines the fact that in the absence of data in the intermediate zone, the latter may be indirectly characterized using the existing field datasets collected in shallow aquifers and at depth in the reservoir. In this shale-dominated succession, important insights into the control of structural discontinuities on fluid circulation can be obtained using these limited datasets. The methodology developed for this study could be applied to other sedimentary basins to address similar issues or other environmental concerns related to deep industrial activities, such as the geological sequestration of carbon dioxide or the use of deep geothermal energy, where potential fluid flow pathways also need to be identified beforehand.

7 Acknowledgments

This project was part of the Environmental Geoscience Program of Natural Resources Canada. It also benefited from funding from the Energy Sector through the Eco-EII and PERD programs. The authors wish to thank the land owners of drilling sites, *Talisman Energy* (now *Repsol Oil and Gas Canada inc.)* and especially Marianne Molgat and Vincent Perron, as well as Charles

Lamontagne of the *Ministère du Développement durable, de l'Environnement et de la Lutte contre les Changements climatiques du Québec*, for providing well logs and seismic data. The authors acknowledge Dr. Stephen Grasby (*GSC*) for reviewing the document. The manuscript was significantly improved by comments and suggestions from Elena Konstantinovskaya, Sylke Hilberg and two anonymous reviewers. This is GSC contribution 20170286.

8 Appendices

Appendix 1 Methods description and limitation for fracture aperture estimations

Fracture apertures estimated in:	Shallow wells using Acoustic Televiewer logs	Deep well B using Formation MicroImager logs
Estimation method	Manual picking on the image log (travel time or amplitude); data from Crow and Ladevèze (2015).	Calculation using resistivity measurements and the addition of current flow caused by the presence of fractures (performed by the logging company using the Luthi and Souhaité (1990) method on well B data)
Factors that limit the quality of apparent aperture estimations (Luthi and Souhaité 1990; Davatzes and Hickman 2010; Ruehlicke 2015)	1) Aperture enhancements due to drilling and borehole orientation. 2) Reduction in acoustic impedance contrasts due to wall roughness. 3) Footprint of the acoustic beam	1) Resistivity contrasts between fracture filling and the host rock. 2) Fracture geometry at the borehole wall (assumptions: planar fractures, infinite length, no cross-cutting fractures, no partial borehole intersection, no edge-effects). 3) Lithology variations over fracture length. 4) Image quality. 5) Electrode button dimensions. 6) Anisotropic *in situ* stress conditions

Appendix 2 Methods used for the calculation of the normal fault core properties of the Rivière Jacques-Cartier fault zone.

The Shale Gouge Ratio (SGR) method (Yielding *et al.* 1997; Freeman *et al.* 1998) (Eqn 5) is based on the length of the throw along the faults (T; i.e. the vertical displacements of the stratigraphic units), the thicknesses of the stratigraphic units (Δz) and the volume of shale (V_{sh}) within these units to estimate the percentage of shale within a portion of the sedimentary succession that has slipped past a certain point along the fault. T and Δz of this normal fault system were identified using the cross-section presented in Fig. 1. Similar estimations were not possible (or would have been speculative at best) in the case of the thrust faults because these structures often display only shale on shale repetitions with little lithological or stratigraphic contrasts. Gamma ray logs were used to estimate V_{sh} (Rider 2002). Séjourné (2015) used a similar approach, employing computed gamma ray logs (called HCGR), acquired in the deep shale gas wells and in conventional wells drilled in the area in the Lorraine Group, Utica Shale, Trenton and Beekmantown groups and an empirical equation for pre-Tertiary rocks proposed by Atlas (1982). The V_{sh} values used in this current exercise are from this dataset: 0.44, 0.21, 0.08 and 0.20 respectively for the Lorraine Group, Utica Shale, Trenton Group and Beekmantown Group. Tightly sealed faults display high SGR values. Threshold values of 18% (Freeman *et al.* 1998) or 20% (Yielding *et al.* 1997) were proposed for sealed faults in shale/sandstone successions that display cross-fault pressure differences.

$$SGR = \frac{\sum\left(V_{sh}.\Delta z\right)}{T}.100 \tag{5}$$

The Sperrevik *et al.* (2002) relationship (Eqn 6) is an empirical relationship developed using core samples collected in faulted clastic reservoirs in the United Kingdom and in the Sinai Desert (Knott *et al.* 1996). These cores include sandstones and some clay-rich units such as shales. Eqn 6 is based on the clay content and of compaction and diagenesis effects which strongly impacts rock porosity and permeability. The maximum burial depth (z_{max}) and the depth at the time of rock deformation/faulting (z_{def}) were used as proxies. This is relevant for the study area as the geological units were buried under at least 5000 m of Paleozoic strata before erosion (Héroux and Bertrand 1991; Yang and Hesse 1993). Then, z_{max} corresponds to the actual depth of the units plus a 5000 m value. Because a conservative estimate was used for the z_{def} value, the shallower depths of the stratigraphic units at the fault footwall were used. The parameter *k* is the fault core permeability expressed in milliDarcies (mD) (1 mD=10^{-15} m^2), *a* are empirical parameters proposed in Sperrevik *et al.* (2002) (a_1=80000; a_2=19.4; a_3=0.00403; a_4= 0.0055; a_5= 12.5). As proposed in the previous section, the use of *k* (m^2 or mD) instead of *K* (m/s) is used here because of the presence of multiple phases in the pore space (water, gas, brines) of the cover succession. For comparison purposes, the *k* values are converted into *K* using the thermo-physical properties of water at 35°C (the temperature estimated at an arbitrary depth of 1500 m using the mean geothermal gradient proposed in Bédard *et al.* (2014) for the SLP).

$$k = a_1.\exp-\left(a_2.V_{sh} + a_3.z_{\max} + \left(a_3.z_{def} - a_5\right)\left(1-V_{sh}\right)^7\right) \qquad (6)$$

Appendix 3 Estimated hydraulic properties: min, geometric mean and max for the values presented in Fig. 6.

	Estimated hydraulic properties		
	Fracture porosity (%)	Hydraulic conductivity *K* (m/s)	Permeability *k* (m^2) (1 m^2=10^{15} mD)
Shallow aquifer	3.50	3.2 $\times 10^{-7}$	4.1 $\times 10^{-12}$
	1.01 / 8.04	2.3 $\times 10^{-9}$ / 1.1 $\times 10^{-5}$	2.9 $\times 10^{-14}$ / 1.4 $\times 10^{-10}$
Intermediate zone (IZ): using apertures	0.45	4.4 $\times 10^{-8}$	5.6 $\times 10^{-13}$
	0.15 / 1.22	1.6 $\times 10^{-9}$ / 8.3$\times 10^{-7}$	2.1 $\times 10^{-14}$ / 1.1 $\times 10^{-11}$
	0.0030	9.4 $\times 10^{-14}$	7.4 $\times 10^{-19}$

from: 1) shallow aquifers 2) lower portion of the IZ:	0.0069 / 0.014	6.2 $\times 10^{-15}$ / 9.2 $\times 10^{-13}$	4.0 $\times 10^{-20}$ / 8.1 $\times 10^{-18}$
Reservoir	0.00070	6.9 $\times 10^{-17}$	3.7 $\times 10^{-22}$
	0.00020 / 0.00084	1.5 $\times 10^{-18}$ / 1.1 $\times 10^{-13}$	7.9 $\times 10^{-24}$ / 6.1 $\times 10^{-19}$

Appendix 4 Open fracture densities for deep wells (fracture densities were calculated using a 15 m window size every 5 m).

		Well A	Well B	Well C
	Distance to the Logan's Line	3 km	9 km	15 km
Open fracture densities (no. fr./m)	Lorraine Group - Vertical portion	0.018	0.014	0.0067
	Utica Shale - Vertical portion	0.006	0	0
	Utica Shale - Horizontal Leg	1.14	0.03	0
	Shallow vertical wells (for comparison)	Up to 1.32 open fractures/meter (Fig. 5)		

References

Atlas D (1982) Well logging and interpretation techniques. The course for home study. Dresser Industries Inc

BAPE (2010) Comparaison des shales d'Utica et de Lorraine avec des shales en exploitation, Réponse de la l'APGQ aux questions de la Commission du BAPE sur les gaz de schiste. Bureau d'Audiences Publiques sur l'Environnement (BAPE) DB25

BAPE (2014) Les enjeux liés à l'exploration et l'exploitation du gaz de schiste dans le shale d'Utica des basses-terres du Saint-Laurent. Rapport d'enquête et d'audience publique. Bureau d'audiences publiques sur l'environnement (BAPE) Bibliothèque et Archives nationales du Québec, Québec City, Canada Report 307: 546

Barton CA, Zoback MD, Moos D (1995) Fluid flow along potentially active faults in crystalline rock. Geology 23: 683-686

Bear J (1993) 1 - Modeling Flow and Contaminant Transport in Fractured RocksFlow and Contaminant Transport in Fractured Rock:1-37.

Bédard K, Raymond J, Malo M, Konstantinovskaya E, Minea V (2014) St. Lawrence Lowlands Bottom-Hole Temperatures: Various Correction Methods. GRC Transactions 38

Bense VF, Van Balen R (2004) The effect of fault relay and clay smearing on groundwater flow patterns in the Lower Rhine Embayment. Basin Research 16: 397-411 DOI 10.1111/j.1365-2117.2004.00238.x

Bense VF, Person MA (2006) faults as conduit-barrier systems to fluid flow in siliclastic sedimentary aquifers. Water Resources Research 42 DOI 10.1029/2005WR004480

Bense VF, Gleeson T, Loveless SE, Bour O, Scibek J (2013) Fault zone hydrogeology. Earth-Science Reviews 127: 171-192 DOI http://dx.doi.org/10.1016/j.earscirev.2013.09.008

Berkowitz B (2002) Characterizing flow and transport in fractured geological media: A review. Advances in Water Resources 25: 861-884 DOI 10.1016/s0309-1708(02)00042-8

Birdsell DT, Rajaram H, Dempsey D, Viswanathan HS (2015) Hydraulic fracturing fluid migration in the subsurface: A review and expanded modeling results. Water Resources Research 51: 7159-7188 DOI 10.1002/2015wr017810

Bordeleau G, Rivard C, Lavoie D, Lefebvre R, Ahad J, Mort A, Xu X (2018a) A multi-isotope approach to determine the origin of methane and higher alkanes in groundwater of the Saint-Édouard area, eastern Canada, submitted to Environmental Geoscience.

Bordeleau G, Rivard C, Lavoie D, Lefebvre R, Malet X, Ladevèze P (2018b) Geochemistry of groundwater in the St-Edouard area, Quebec, Canada, and its influence on the distribution of methane in the aquifers. Applied Geochemistry 89: 92-108 DOI https://doi.org/10.1016/j.apgeochem.2017.11.012

Borghi A, Renard P, Courrioux G (2015) Generation of 3D Spatially Variable Anisotropy for Groundwater Flow Simulations. Groundwater: n/a-n/a DOI 10.1111/gwat.12295

Bossennec C, G├⌐raud Y, Moretti I, Mattioni L, Stemmelen D (2018) Pore network properties of sandstones in a fault damage zone. Journal of Structural Geology 110: 24-44 DOI https://doi.org/10.1016/j.jsg.2018.02.003

Bowker KA (2007) Barnett Shale gas production, Fort Worth Basin: issues and discussion. AAPG Bulletin 91: 523-533

Caine JS, Evans JP, Forster CB (1996) Fault zone architecture and permeability structure. Geology 24: 1025-1028 DOI 10.1130/0091-7613(1996)024<1025:fzaaps>2.3.co;2

Castonguay S, Dietrich J, Shinduke R, Laliberté J-Y (2006) Nouveau regard sur l'architecture de la Plate-forme du Saint-Laurent et des Appalaches du sud du Québec par le retraitement des profils de sismique réflexion M-2001, M-2002 et M-2003. Commission géologique du Canada, Dossier Public 5328: 19p

CCA (2014) Environmental impacts of shale gas extraction in Canada. Council of Canadian Academies (CCA): 292p

Chatellier J-Y, Flek P, Molgat M, Anderson I, Ferworn K, Lazreg Larsen N, Ko S (2013) Chapter 3: Overpressure in Shale Gas: When Geochemistry and Reservoir Engineering Data Meet and Agree. AAPG Special Volumes Memoir 103: Critical Assessment of Shale Resource Plays, 2013: 45-69

Chen Z, Lavoie D, Malo M, Jiang C, Sanei H, H.Ardakani O (2017) A dual-porosity model for evaluating petroleum resource potential in unconventional tight-shale plays with application to Utica Shale, Quebec (Canada). Marine and Petroleum Geology 80: 333-348 DOI http://dx.doi.org/10.1016/j.marpetgeo.2016.12.011

Clark TH (1964) Région d'Upton. Ministère des Richesses Naturelles, Service d'Exploration Géologique, Rapport Géologique 100

Clark TH, Globensky Y (1973) Portneuf et parties de St-Raymond et de Lyster - Comtés de Portneuf et de Lotbinière. Ministère des Richesses Naturelles, Direction Générale des Mines, Rapport Géologique 148

Crow HL, Ladevèze P (2015) Downhole geophysical data collected in 11 boreholes near St.-Édouard-de-Lotbinière, Québec. Geological Survey of Canada, Open File 7768: 48p. DOI 10.4095/297047

Davatzes NC, Hickman SH (2010) Stress, fracture, and fluid-flow analysis using acoustic and electrical image logs in hot fractured granites of the Coso geothermal field, California, USA., in Proceedings World Geothermal Congress 2010. Bail, Indonesia, 25-29 April 2010.

Dusseault M, Jackson R (2014) Seepage pathway assessment for natural gas to shallow groundwater during well stimulation, in production, and after abandonment. Environmental Geosciences 21: 107-126

EPA (2016) Hydraulic Fracturing for Oil and Gas: Impacts from the Hydraulic Fracturing Water Cycle on Drinking Water Resources in the United States (Final Report). US Environmental Protection Agency (EPA), Washington, DC EPA/600/R-16/236F: 666

Farrell NJC, Healy D (2017) Anisotropic pore fabrics in faulted porous sandstones. Journal of Structural Geology 104: 125-141 DOI https://doi.org/10.1016/j.jsg.2017.09.010

Ferrill DA, Winterle J, Wittmeyer G, Sims D, Colton S, Armstrong A, Morris AP (1999) Stressed rock strains groundwater at Yucca Mountain, Nevada. GSA today 9: 1-8

Freeman B, Yielding G, Needham DT, Badley ME (1998) Fault seal prediction: the gouge ratio method. Geological Society, London, Special Publications 127: 19-25 DOI 10.1144/gsl.sp.1998.127.01.03

Gale J, Ukar E, Elliott SJ, Wang Q (2015) Bedding-Parallel Fractures in Shales: Characterization, Prediction and ImportanceAAPG Annual Convention and Exhibition, Denver, CO., USA, May 31 - June 3, 2015.

Gale JF, Reed RM, Holder J (2007) Natural fractures in the Barnett Shale and their importance for hydraulic fracture treatments. AAPG Bulletin 91: 603-622

Gassiat C, Gleeson T, Lefebvre R, McKenzie J (2013) Hydraulic fracturing in faulted sedimentary basins: Numerical simulation of potential contamination of shallow aquifers over long time scales. Water Resources Research 49: 8310-8327 DOI 10.1002/2013wr014287

Globensky Y (1987) Géologie des Basses Terres du Saint-Laurent. Direction Générale de l'Exploration Géologique et minérale du Québec, Gouvernement du Québec MM 85-02

Grasby SE, Ferguson G, Brady A, Sharp C, Dunfield P, McMechan M (2016) Deep groundwater circulation and associated methane leakage in the northern Canadian Rocky Mountains. Applied Geochemistry 68: 10-18 DOI https://doi.org/10.1016/j.apgeochem.2016.03.004

Haeri-Ardakani O, Sanei H, Lavoie D, Chen Z, Jiang C (2015) Geochemical and petrographic characterization of the Upper Ordovician Utica Shale, southern Quebec, Canada. International Journal of Coal Geology 138: 83-94 DOI http://dx.doi.org/10.1016/j.coal.2014.12.006

Héroux Y, Bertrand R (1991) Maturation thermique de la matière organique dans un bassin du Paléozoïque inférieur, Basses-Terres du Saint-Laurent, Québec, Canada. Canadian Journal of Earth Sciences 28: 1019-1030

Jackson RE, Gorody AW, Mayer B, Roy JW, Ryan MC, Van Stempvoort DR (2013) Groundwater Protection and Unconventional Gas Extraction: The Critical Need for Field-Based Hydrogeological Research. Groundwater 51: 488-510 DOI 10.1111/gwat.12074

Janos D, Molson J, Lefebvre R (2018) Regional groundwater flow dynamics and residence times in Chaudière-Appalaches, Québec, Canada: Insights from numerical simulations. Canadian Water Resources Journal: 26 DOI 10.1080/07011784.2018.1437370

Kissinger A, Helmig R, Ebigbo A, Class H, Lange T, Sauter M, Heitfeld M, Klünker J, Jahnke W (2013) Hydraulic fracturing in unconventional gas reservoirs: risks in the geological system, part 2. Environmental Earth Sciences 70: 3855-3873 DOI 10.1007/s12665-013-2578-6

Knott SD, Beach A, Brockbank PJ, Lawson Brown J, McCallum JE, Welbon AI (1996) Spatial and mechanical controls on normal fault populations. Journal of Structural Geology 18: 359-372 DOI http://dx.doi.org/10.1016/S0191-8141(96)80056-3

Konstantinovskaya E, Rodriguez D, Kirkwood D, Harris L, Thériault R (2009) Effects of basement structure, sedimentation and erosion on thrust wedge geometry: an example from the Quebec Appalachians and analogue models. Bulletin of Canadian Petroleum Geology 57: 34-62

Konstantinovskaya E, Malo M, Castillo DA (2012) Present-day stress analysis of the St. Lawrence Lowlands sedimentary basin (Canada) and implications for caprock integrity during CO2 injection operations. Tectonophysics 518-521: 119-137 DOI 10.1016/j.tecto.2011.11.022

Konstantinovskaya E, Malo M, Badina F (2014a) Effects of irregular basement structure on the geometry and emplacement of frontal thrusts and duplexes in the Quebec Appalachians: Interpretations from well and seismic reflection data. Tectonophysics 637: 268-288 DOI http://dx.doi.org/10.1016/j.tecto.2014.10.012

Konstantinovskaya E, Rutqvist J, Malo M (2014b) CO2 storage and potential fault instability in the St. Lawrence Lowlands sedimentary basin (Quebec, Canada): Insights from coupled reservoir-geomechanical modeling. International Journal of Greenhouse Gas Control 22: 88-110 DOI http://dx.doi.org/10.1016/j.ijggc.2013.12.008

Ladevèze P, Rivard C, Lefebvre R, Lavoie D, Parent M, Malet X, Bordeleau G, Gosselin J-S (2016) Travaux de caractérisation hydrogéologique dans la plateforme sédimentaire du Saint-Laurent, région de Saint-Édouard-de-Lotbinière, Québec. Commission géologique du Canada, Dossier Public 8036: 112 DOI 10.4095/297891

Ladevèze P, Séjourné S, Rivard C, Lefebvre R, Lavoie D, Rouleau A (2018) Defining the natural fracture network in a shale gas play and its cover succession; the case of the Utica Shale in eastern Canada. Journal of Structural Geology 108: 157-170 DOI https://doi.org/10.1016/j.jsg.2017.12.007

Laubach SE (2003) Practical approaches to identifying sealed and open fractures. AAPG Bulletin 87: 561-579

Laubach SE, Olson JE, Gale JFW (2004) Are open fractures necessarily aligned with maximum horizontal stress? Earth and Planetary Science Letters 222: 191-195 DOI http://dx.doi.org/10.1016/j.epsl.2004.02.019

Lavoie D (2008) Chapter 3 Appalachian Foreland Basin of Canada. In: Andrew DM (ed) Sedimentary Basins of the World:65-103.

Lavoie D, Hamblin AP, Theriault R, Beaulieu J, Kirkwood D (2008) The Upper Ordovician Utica Shales and Lorraine Group flysch in southern Québec: Tectonostratigraphic setting and significance for unconventional gas. Commission géologique du Canada, Open File 5900: 56

Lavoie D, Desrochers A, Dix G, Knight I, Salad Hersi O (2012) The Great American Carbonate Bank in Eastern Canada: An Overview. In: Derby, J.R., Fritz, R.D., Longacre, S.A., Morgan, W.A., Sternbach, C.A. (Eds.), The Great American Carbonate Bank. The Geology and Economic Resources of the Cambrian–Ordovician Sauk Megasequence of Laurentia. AAPG Memoirs 98: 499-523

Lavoie D, Rivard C, Lefebvre R, Séjourné S, Thériault R, Duchesne MJ, Ahad JME, Wang B, Benoit N, Lamontagne C (2014) The Utica Shale and gas play in southern Quebec: Geological and hydrogeological syntheses and methodological approaches to groundwater risk evaluation. International Journal of Coal Geology 126: 77-91 DOI http://dx.doi.org/10.1016/j.coal.2013.10.011

Lavoie D, Pinet N, Bordeleau G, Ardakani OH, Ladevèze P, Duchesne MJ, Rivard C, Mort A, Brake V, Sanei H, Malet X (2016) The Upper Ordovician black shales of southern Quebec (Canada) and their significance for naturally occurring hydrocarbons in shallow groundwater. International Journal of Coal Geology 158: 44-64 DOI http://dx.doi.org/10.1016/j.coal.2016.02.008

Lefebvre R (2016) Mechanisms leading to potential impacts of shale gas development on groundwater quality. Wiley Interdisciplinary Reviews: Water DOI 10.1002/wat2.1188

Lehner FK, Pilaar WF (1997) The emplacement of clay smears in synsedimentary normal faults: inferences from field observations near Frechen, Germany. In: Moller-Pedersen P, Koestler AG (eds) Norwegian Petroleum Society Special Publications:39-50.

Luthi SM, Souhaite P (1990) Fracture apertures from electrical borehole scans. Geophysics 55: 821-833 DOI 10.1190/1.1442896

Luthi SM, Souhaité P (1990) Fracture apertures from electrical borehole scans. Geophysics 55: 821-833

Manzocchi T, Walsh J, Nell P, Yielding G (1999) Fault transmissibility multipliers for flow simulation models. Petroleum Geoscience 5: 53-63

Martini AM, Walter LM, Budai JM, Ku TCW, Kaiser CJ, Schoell M (1998) Genetic and temporal relations between formation waters and biogenic methane: Upper Devonian Antrim Shale, Michigan Basin, USA. Geochimica et Cosmochimica Acta 62: 1699-1720 DOI http://dx.doi.org/10.1016/S0016-7037(98)00090-8

Méheust Y, Schmittbuhl J (2001) Geometrical heterogeneities and permeability anisotropy of rough fractures. Journal of Geophysical Research: Solid Earth 106: 2089-2102 DOI 10.1029/2000jb900306

Moreno L, Tsang C-F, Tsang Y, Neretnieks I (1990) Some anomalous features of flow and solute transport arising from fracture aperture variability. Water Resources Research 26: 2377-2391 DOI 10.1029/WR026i010p02377

Morin C (1991) Rapport de qualification, poursuite des travaux d'exploration Villeroy. In: SIGPEG (ed), pp. 52.

Mortimer L, Aydin A, Simmons CT, Love AJ (2011) Is in situ stress important to groundwater flow in shallow fractured rock aquifers? Journal of Hydrology 399: 185-200 DOI 10.1016/j.jhydrol.2010.12.034

Nowamooz A, Lemieux JM, Therrien R (2013) Étude E3-10, Modélisation numérique de la migration du méthane dans les Basses-Terres du Saint-Laurent. Rapport final. Département de géologie et de génie géologique, Université Laval: 115

Oda M (1985) Permeability tensor for discontinuous rock masses. Geotechnique 35: 483-495 DOI 10.1680/geot.1985.35.4.483

Oda M (1988) A method for evaluating the representative elementary volume based on joint survey of rock masses. Canadian Geotechnical Journal 25: 440-447 DOI 10.1139/t88-049

Odling NE, Gillespie P, Bourgine B, Castaing C, Chiles JP, Christensen NP, Fillion E, Genter A, Olsen C, Thrane L, Trice R, Aarseth E, Walsh JJ, Watterson J (1999) Variations in fracture system geometry and their implications for fluid flow in fractures hydrocarbon reservoirs. Petroleum Geoscience 5: 373-384 DOI 10.1144/petgeo.5.4.373

Odling NE, Harris SD, Knipe RJ (2004) Permeability scaling properties of fault damage zones in siliclastic rocks. Journal of Structural Geology 26: 1727-1747 DOI https://doi.org/10.1016/j.jsg.2004.02.005

Ortoleva P, Al-Shaieb Z, Puckette J (1995) Genesis and dynamics of basin compartments and seals. American Journal of Science 295: 345-427 DOI 10.2475/ajs.295.4.345

Osborne MJ, Swarbrick RE (1997) Mechanisms for generating overpressure in sedimentary basins: a reevaluation. AAPG Bulletin 81: 1023-1041

Peacock DCP, Nixon CW, Rotevatn A, Sanderson DJ, Zuluaga LF (2016) Glossary of fault and other fracture networks. Journal of Structural Geology 92: 12-29 DOI http://dx.doi.org/10.1016/j.jsg.2016.09.008

Reagan MT, Moridis GJ, Keen ND, Johnson JN (2015) Numerical simulation of the environmental impact of hydraulic fracturing of tight/shale gas reservoirs on near-surface groundwater: Background, base cases, shallow reservoirs, short-term gas, and water transport. Water Resources Research 51: 2543-2573 DOI 10.1002/2014wr016086

Rider M (2002) The geological interpretation of well logs. Second Edition Rider-French Consulting Ltd.

Rodrigues N, Cobbold PR, Loseth H, Ruffet G (2009) Widespread bedding-parallel veins of fibrous calcite ('beef') in a mature source rock (Vaca Muerta Fm, Neuquén Basin, Argentina): evidence for overpressure and horizontal compression. Journal of the Geological Society 166: 695-709 DOI 10.1144/0016-76492008-111

Ruehlicke B (2015) From Borehole Images to Fracture Permeability and Fracturing Pressure. Oral presentation given at Geoscience Technology Workshop, Unconventionals Update, Austin, Texas, November 4-5, 2014

Séjourné S, Dietrich J, Malo M (2003) Seismic characterization of the structural front of southern Quebec Appalachians. Bulletin of Canadian Petroleum Geology 51: 29-44 DOI 10.2113/51.1.29

Séjourné S, Lefebvre R, Malet X, Lavoie D (2013) Synthèse géologique et hydrogéologique du Shale d'Utica et des unités sus-jacentes (Lorraine, Queenston et dépots meubles), Basses-Terres du Saint-Laurent, Québec. Commission Géologique du Canada, Dossier Public 7338: 165 DOI 10.4095/292430

Séjourné S (2015) Caractérisation des réseaux de fractures naturelles, de la porosité et de la saturation en eau du Shale d'Utica et de sa couverture par l'analyse des diagraphies de forages pétroliers dans la région de Saint-Édouard, Québec. Commission Géologique du Canada, Dossier Public 7980: 60 DOI 10.4095/297473

Séjourné S (2017) Étude géomécanique du Shale d'Utica et de sa couverture d'après les puits pétroliers et gaziers de la région de Saint-Édouard-de-Lotbinière, Québec. Commission Géologique du Canada, Dossier Public 8196: 54 DOI 10.4095/299662

Sibson R (1977) Fault rocks and fault mechanisms. Journal of the Geological Society 133: 191-213

Slivitzky A, St-Julien P (1987) Compilation géologique de la région de l'Estrie-Beauce Direction Générale de l'Exploration Géologique et minérale du Québec - Gouvernement du Québec.

Snow DT (1968) Rock fracture spacings, openings, and porosities. Journal of Soil Mechanics & Foundations Div

Sperrevik S, Faerseth RB, Gabrielsen RH (2000) Experiments on clay smear formation along faults. Petroleum Geoscience 6: 113-123

Sperrevik S, Gillespie PA, Fisher QJ, Halvorsen T, Knipe RJ (2002) Empirical estimation of fault rock properties. In: Andreas GK, Robert H (eds) Norwegian Petroleum Society Special Publications:109-125.

St-Julien P, Hubert C (1975) Evolution of the Taconian orogen in the Quebec Appalachians. American Journal of Science 275-A: 337-362

St-Julien P, Slivitsky A, Feininger T (1983) A deep structural profile across the Appalachians of southern Quebec. Geological Society of America Memoirs 158: 103-112 DOI 10.1130/MEM158-p103

Terzaghi RD (1965) Sources of error in joint surveys. Geotechnique 15 (3): 287-304

Thériault R, Beauséjour S (2012) Carte géologique du Québec, Edition 2012. Ressources Naturelles Québec DV 2012-07

Thompson LB (2009) Atlas of borehole imagery AAPG/Datapages

Tran Ngoc TD, Lefebvre R, Konstantinovskaya E, Malo M (2014) Characterization of deep saline aquifers in the Bécancour area, St. Lawrence Lowlands, Québec, Canada: implications for CO2 geological storage. Environmental Earth Sciences: 1-28 DOI 10.1007/s12665-013-2941-7

Tremblay A, Pinet N (2016) Late Neoproterozoic to Permian tectonic evolution of the Quebec Appalachians, Canada. Earth-Science Reviews 160: 131-170 DOI http://dx.doi.org/10.1016/j.earscirev.2016.06.015

Tsang C-F, Neretnieks I (1998) Flow channeling in heterogeneous fractured rocks. Reviews of Geophysics 36: 275-298 DOI 10.1029/97rg03319

Vrolijk PJ, Urai JL, Kettermann M (2016) Clay smear: Review of mechanisms and applications. Journal of Structural Geology 86: 95-152 DOI http://dx.doi.org/10.1016/j.jsg.2015.09.006

Watts NL (1987) Theoretical aspects of cap-rock and fault seals for single- and two-phase hydrocarbon columns. Marine and Petroleum Geology 4: 274-307 DOI http://dx.doi.org/10.1016/0264-8172(87)90008-0

Weber KJ, Mandl GJ, Pilaar WF, Lehner BVF, Precious RG (1978) The Role Of Faults In Hydrocarbon Migration And Trapping In Nigerian Growth Fault Structures, 1978/1/1 1978

Witherspoon PA, Wang JSY, Iwai K, Gale JE (1980) Validity of Cubic Law for fluid flow in a deformable rock fracture. Water Resources Research 16: 1016-1024 DOI 10.1029/WR016i006p01016

Wladis D, Jönsson P, Wallroth T (1997) Regional characterization of hydraulic properties of rock using well test dataSwedish Nuclear Fuel and Waste Management Co (SKB) Technical Report Department of Geology, Charlmers University of Technology, Göteborg Sweden, pp. 54.

Yang C, Hesse R (1993) Diagenesis and anchimetamorphism in an overthrust belt, external domain of the Taconian Orogen, southern Canadian Applachians-II. Paleogeothermal gradients derived from maturation of different types of organic matter. Organic Geochemistry 20: 381-403 DOI http://dx.doi.org/10.1016/0146-6380(93)90127-W

Yielding G, Freeman B, Needham DT (1997) Quantitative fault seal prediction. AAPG Bulletin 81: 897-917

Zoback MD (2010) Reservoir Geomechanics. Cambridge University Press. 449p.